2007

Investigation of the Reflective Properties of a Left-Handed Metamaterial

Amanda Durham
Wright State University

INVESTIGATION OF THE REFLECTIVE PROPERTIES

OF A LEFT-HANDED METAMATERIAL

A thesis submitted in partial fulfillment
of the requirements for the degree of
Master of Science

By

AMANDA DURHAM
B.S., Embry-Riddle Aeronautical University, 2004

2007
Wright State University

WRIGHT STATE UNIVERSITY

SCHOOL OF GRADUATE STUDIES

March 29, 2007

I HEREBY RECOMMEND THAT THE THESIS PREPARED UNDER MY SUPERVISION BY Amanda Durham ENTITLED Investigation of the Reflective Properties of a Left-handed Metamaterial BE ACCEPTED IN PARTIAL FULFILLMENT OF THE REQUIREMENTS FOR THE DEGREE OF Master of Science.

_____

Lok Lew Yan Voon, Ph.D.
Thesis Advisor

_____

Lok Lew Yan Voon, Ph.D.
Department Chair

Committee on
Final Examination

_____

Lok Lew Yan Voon, Ph.D.

_____

Gregory Kozlowski, Ph.D.

_____

Douglas Petkie, Ph.D.

_____

Joseph F. Thomas, Jr., Ph.D.
Dean, School of Graduate Studies

Abstract

Durham, Amanda, M.S., Department of Physics, Wright State University,
2007. Investigation of the Reflective Properties of a Left-handed Metamaterial.

The purpose of this project is to investigate the reflective properties of a left-handed metamaterial (LHM) through the use of a finite element analysis software called FEMLAB. In the 1960's, V. Veselago theorized that a material with negative permeability and negative permittivity has a negative index of refraction. In 2000, such a metamaterial was built and demonstrated at microwave frequencies.

Previous work had focused on the transmission properties of the metamaterial. In our work, the reflected wave was examined for a LHM subject to an incident transverse electric wave. The different generalizations, first proposed by Veselago, of the Fresnel and Snell's equations for LHM's were rederived. We show that the reflectance does not distinguish between normal materials and metamaterials, and, through computational results, that FEMLAB can be used for LHM's.

Contents

Page

Figures

Page

Tables

Page

1 INTRODUCTION

The name and theory of left-handed materials (LHM), whose properties include negative permeability, negative permittivity, and hence a negative index of refraction, were created by Veselago in 1968 [1]. Since the late 1960's the theories of LHM's blossomed, but it was not until recently that the theories became a reality in the laboratories. Before presenting current available literature and future paths for a LHM, I would like to explain the physical properties of a LHM. There are many areas in the industry that a LHM can be used in, such as optics, acoustics, weather, national security, medicine, etc, but in this report only the optics field will be inspected and explained.

1.1 Definition of a Left-Handed Metamaterial

A metamaterial is a man-made material. A left-handed material is a material whose physical properties cause **E**, **H**, and **k** to form a left-handed triple of vectors [2]. Assuming an isotropic medium, the ray diagram for an interface between a medium with a positive index of refraction and a LHM can be seen in Figure 1 below.

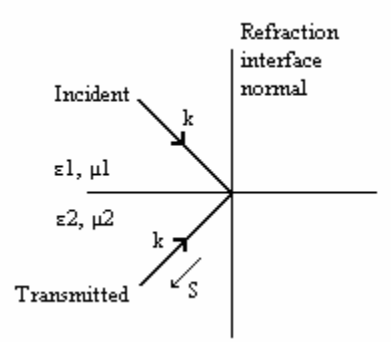

Figure 1: Ray diagram of interface between n>0 and n<0 media

The diagram in Figure 1 can be explained using Snell's law, $\frac{\sin\theta_i}{\sin\theta_r} = n_{21} = \frac{n_2}{n_1}$, where θ_r defines the angle between the ray and refraction interface normal. A later section includes an explanation to the corrected Snell's law. For the case where $n>1$ for both media, the ray would pass through the interface, where it would bend either towards or away from the normal, but never continue propagating on the same side of the normal as the incoming wave. Since, in this case, the indices of refraction include $n_1>0$ and $n_2<0$, the transmitted ray travels through the second medium on the same side of the normal as the incident wave [3]. The resulting wave is what is called a backwards moving wave (BW). The physical properties of a BW require that the Poynting vector, S, points in the direction of energy flow and continues in the proper direction, but the wave vector propagates in the negative direction.

The physical properties of the material must include a permittivity, ε, and permeability, μ, less than zero in order to obtain a negative index of refraction, n. The relationship between ε, μ, and n is defined as $n = \pm\sqrt{\varepsilon\mu}$. As long as both ε and μ values are real and

negative, the product will be real and positive but the refractive index will be real and negative. This means that propagating modes will exist. Smith and coworkers have shown that the $n<0$ solution is correct and is not rejected on the grounds of causality [4].

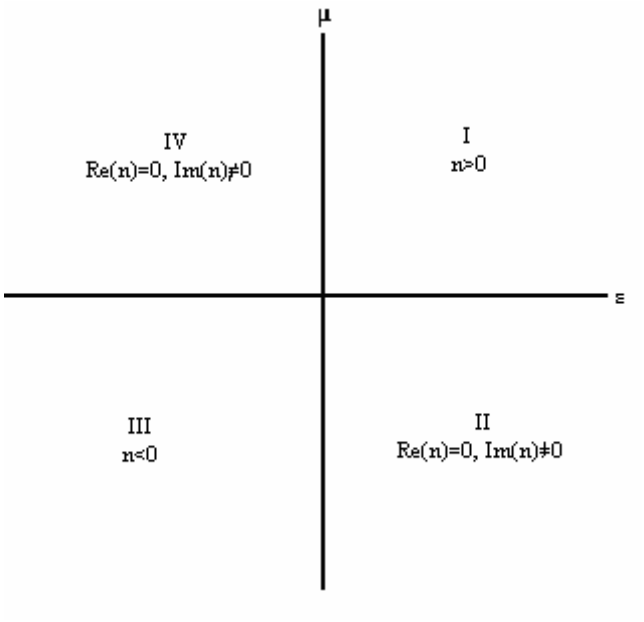

Figure 2: All possible combinations for ε and μ

Figure 2 shows all the various combinations for ε and μ [2]. Quadrant I symbolizes materials whose ε, $\mu>0$, which means $n>0$. Quadrant III represents a LHM, where both ε, $\mu<0$ and therefore $n<0$, this is the quadrant that will be focused on during this report. Quadrants II and IV represent the situation where either ε or $\mu<0$ and these material's properties do not permit electromagnetic waves to propagate through them [2].

1.2 A Different Backwards Wave Source

If an anisotropic medium, whose physical properties include $\varepsilon<0$ and $\mu<0$, is used, a BW is also formed. However, in this case the BW is caused by the group velocity and phase velocity moving in opposite directions. The phase velocity is the speed at which the actual wave moves, while the group velocity is the speed at which the wave packet moves. Figure 3 below helps to visualize the wave movement in this situation. This phenomenon is the result of change in the group velocity's envelope as it moves through the dispersive medium. Before explaining the velocity equations for an anisotropic material, the velocity equations for an isotropic material must be explained.

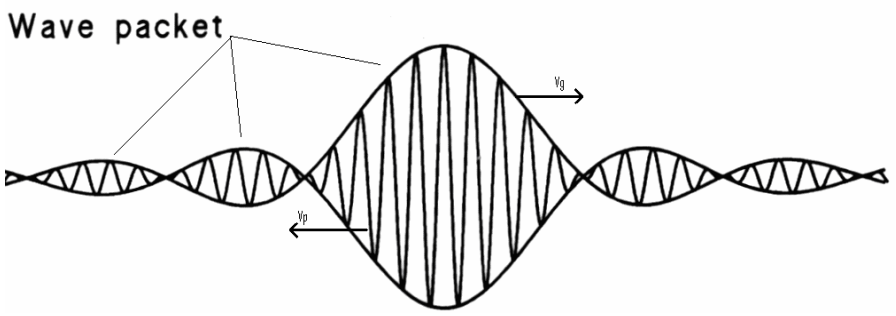

Figure 3: Example of group and phase velocities moving in opposite directions

A 1-D example can be used to show that when a wave moves through a nondispersive medium the group velocity is equal to the phase velocity as there is no phase change. First, however, a few assumptions must be made:

1. These are time harmonic waves.
2. The wave has its own wavelength, which moves the entire wavelength in one period.

3. The amplitude does not grow.

After looking at the assumptions, the wave can be defined as $u(x,t) = u_0 \sin(kx - \omega t)$, where $k = |k| = \text{wave number} = \omega/v = 2\pi/\lambda$. Since there is no phase change, the group velocity is defined as $v_g = \omega/k$, and therefore $v_g = v_p$. Even if a pulsed wave is introduced into an isotropic medium, the group and phase velocities will remain the same.

Looking at two instances in time, the wave defining equations can be written as,

$$\begin{aligned} u_1(x,t) &= u_0 \sin(k'x - \omega' t) \\ u_2(x,t) &= u_0 \sin(kx - \omega t) \end{aligned}, \text{ where } u(x,t) = u_1 + u_2, \qquad (1.1.1.1)$$

$$\therefore u(x,t) \approx 2u_0 \cos\{\tfrac{1}{2}((k'-k)x - (\omega'-\omega)t\} \sin(kx - \omega t). \qquad (1.1.1.2)$$

The values within the curly brackets define the modulated amplitude of the sine function. Note that the sine function has its own group velocity equal to $v_g = (\omega'-\omega)/(k'-k) \approx d\omega/dk$. The phase velocity for a dispersive medium, where $\omega = kv$, is defined as $v_g = v_p + k\, dv/dk$. For a LHM, where the wave vector is referring back to the definitions for v_p and v_g above, the wave packet will be moving in the opposite direction from the wave [3].

1.3 Report Explanation

The first step to explaining the simulation used in this paper involves returning to Figure 2 above and setting the properties of medium one to those of air and medium two's

physical properties to those of a glass slab with a negative index of refraction. Figure 4 below represents the geometry that will be used throughout the rest of this paper.

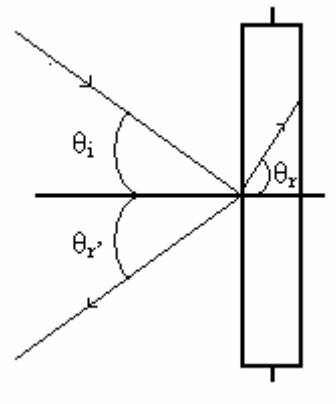

Figure 4: Diagram of geometry used for paper

The purpose of this paper is to examine the reflective properties of a LHM, more specifically a glass slab with a negative index of refraction. Much of the published material using the "super lens" concept investigates the transmissive properties of a LHM. There are fewer articles exploring the results of $n<0$ and the effects these physical properties may have on the reflectance values of a medium [6-9]. Through the use of a finite element method software called FEMLAB, I am able to produce an electric field incident on the glass slab and calculate what percentage of the field is reflected. Reflectance values are determined through the use of Fabry-Perot equations.

2 LITERATURE REVIEW

Although Veselago's first publication dealing with LHM occurred in 1968, he has continued theorizing over the years. In some publications he has made corrections to his own theories and in some he has challenged the work of other scientists. In a recent publication, Veselago et al. stated that if both negative permeability and permittivity are present in a material, **E**, **H**, and **k** form a left-handed triple of vectors and hence, the group and phase velocity are moving in antiparallel directions [2].

2.1 Examples of LHM

In the last few years, multiple books have been published that are completely dedicated to discussing a negative index of refraction and metamaterials [10, 11]. Though these publications are important to scientific community, the biggest leap occurred when the LHM went from theory to reality. Since the glass slab model is presented in great detail throughout this report, other types of LHM will be discussed here. Many scientists have presented both theoretical and experimental results on LHM's made of such objects as split-ring resonators (SRR) and lattices composed of very thin rods. For both cases, the conducting elements of the array are effective when the wavelength is much larger than the element dimension and lattice spacing [12].

2.1.1 Split-ring resonators (SRR)

A SRR is a cylinder made of thin sheets tightly wound around each other as shown in Figure 5. Note that there is a gap which does not allow the sheets to create a complete circle.

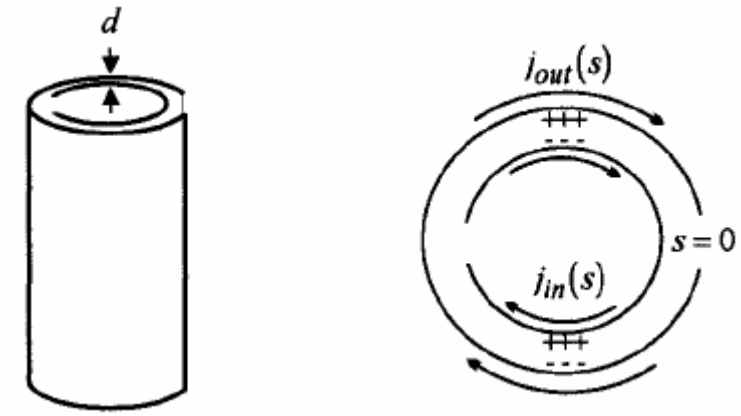

Figure 5: Coils of SRR (left) and representation current flow of a SRR (right)

Using the physical properties described by Pendry, a current can be induced in the SRR when a magnetic field is introduced parallel to the cylinder [13]. The capacitance between the layers of the SRR also has a direct effect on the current, the larger the capacitance, the greater the current. The tightly wound coils will be used to create an array within a material. The gap within the SRR's circumference, keeps the current from flowing just around one ring.

2.1.2 Thin rod array

Similar to the SRR, another source of LHM properties can be found in a square array of metallic rods, as shown in Figure 6 below, embedded within a medium.

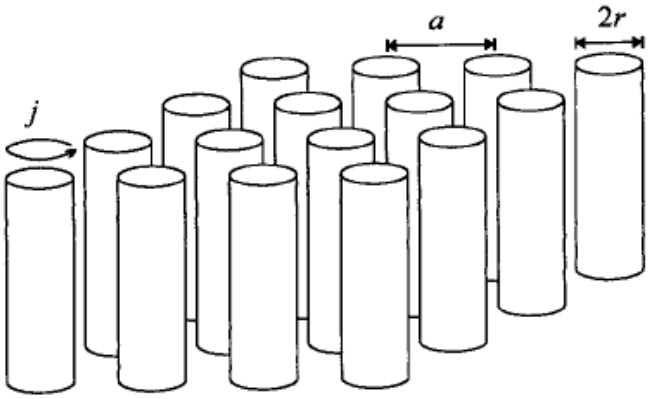

Figure 6: Array of thin rods

Introducing a magnetic field parallel to the rods allows a current, j, to flow around the rods.

2.2 Recent Research

Using structures, such as the ones described above, have allowed scientists to investigate new scenarios and new uses for LHM's. One of the areas of current interest is to break the barriers of frequency dependence. Many experiments have attempted, some have succeeded, to look at the effects of an LHM at higher frequencies and therefore smaller wavelengths [14]. For example, a SRR array was used to experimentally inspect the results of an LHM in the near infrared and optical wavelengths. Results of this experiment were found to agree with the expected results determined through wave analysis [15].

Not long ago, Pendry suggested the idea of a super lens, using the theories of Veselago, which would result in the amplification of evanescent waves in the LHM. Such an

amplification would allow a perfect focus, hence the name "perfect lens." A ray diagram showing the focus of a LHM is shown in Figure 7 [16]. Smith et al. supported Pendry's work by publishing their theory that a slab of LHM would enhance the evanescent waves as they traveled through the medium, and therefore no losses would occur during transmission [5]. However, Pendry's material assumed no reflection at the material interface through positive impedance. Such assumptions support wave transmission [9].

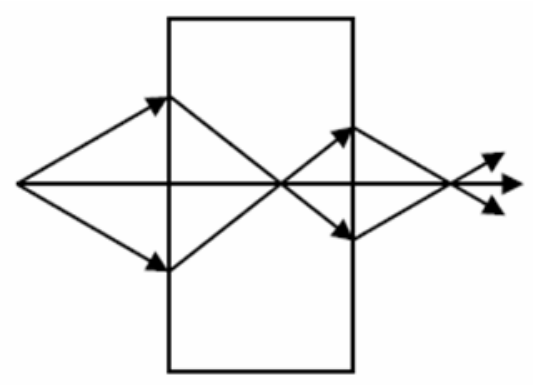

Figure 7: Ray diagram of LHM

More recently, many scientists have theorized and proven that Pendry's theory on wave transmission is not completely accurate due to the fact that nonrealistic material properties were used in the original calculations. For instance, Veselago stated that the classical diffraction limit can not be valid for the Pendry's suggested "super lens" due to the fact that assumed wave conditions in the "super lens" break the uncertainty principle by overcoming the diffraction limit [2]. Lischialpo et al., determined, through a computational experiment, that the focusing of a line source by a LHM does occur but is not perfect [8]. In the case of this report, the existence of a "perfect lens" will not be

pursued, however, the reflective properties of a LHM glass slab will be. The glass lens reflective properties will be addressed and investigated through the use of Fabry-Perot equations and FEMLAB.

Most recently, LHM have been used in the laboratory to "cloak" an object and cause it to be "invisible" to the eye [17]. This goal was achieved by creating a cloak of SRR's that hid a copper cylinder within its circumference. The experimental setup is shown in Figure 8, and Figure 9 shows how the incident wave moves around the inner object to create a cloak [17].

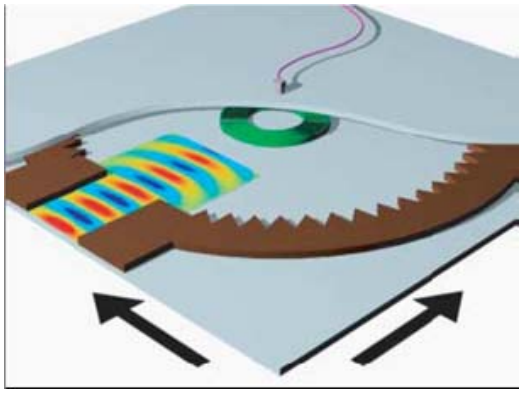

Figure 8: Setup used by Schurig and coworkers during cloaking experiment

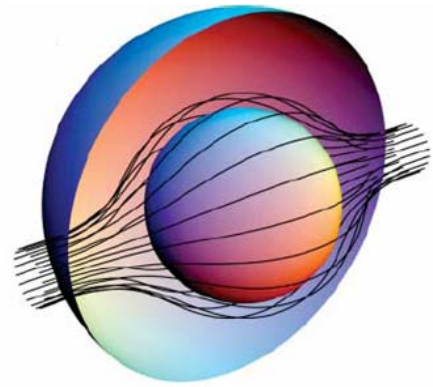

Figure 9: Diagram of cloak and electromagnetic waves

Experimental results proved that cloaking is possible in the microwave region by decreasing the scattering and reducing the object shadow. This combination resembled empty space and hid the cylinder from the observer [17].

3 BACKGROUND

The following sections will give a better insight to how the physical properties of an LHM are defined and the computational methods used to solve for an LHM's defining equations.

3.1 Maxwell's Equations

Although Veselago's theory about an LHM might have been new in the 1960's, the defining equations were not. All of an LHM's physical properties can be defined by or derived from Maxwell's equations. Maxwell's equations, given in Table 1, are part of the fundamentals of electromagnetics and relate the electric and magnetic fields to each other through the use of the four equations below:

$\nabla \times \vec{B} = \mu_0 \vec{J} + \frac{1}{c^2}\frac{\partial \vec{E}}{\partial t}$	Maxwell-Ampere's Law
$\nabla \cdot \vec{E} = \frac{\rho_f}{\varepsilon_0}$	Gauss's Law
$\nabla \times \vec{E} = -\frac{\partial \vec{B}}{\partial t}$	Faraday's Law of Induction
$\nabla \cdot \vec{B} = 0$	Gauss's Law for Magnetism

Table 1: Maxwell's Equations

The equations given above are generalized and need the following relations to define Maxwell's equations for a dielectric

$$\begin{aligned} \vec{D} &= \varepsilon \vec{E}, \\ \vec{B} &= \mu \vec{H}, \\ \varepsilon &= \varepsilon_0 (1 + \chi_e), \\ \mu &= \mu_0 (1 + \chi_m). \end{aligned} \tag{3.1.1}$$

3.2 Physical Property Choices for this Report

3.2.1 LHM vs. photonic crystal

Although a photonic crystal (PC) can be classified as a type of LHM it has very different physical properties than a traditional LHM. A PC is generally a periodic dielectric structure with a lattice spacing shown below.

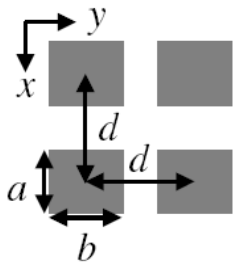

Figure 10: Symmetric lattice structure for a photonic crystal

However the optical properties of a PC can be altered by varying the lattice spacing throughout the structure.

The properties of a traditional LHM are called relative permittivity and permeability and are specific for each node or group of nodes within the lattice. If such a LHM is used a

wavelength much less than the dielectric width should be used to ensure that each node/group in the lattice is taken into account during the calculations.

Due to the lattice spacing of a PC and the inconsistency of the physical properties that may occur throughout the lattice, a PC's physical properties are looked at as effective values that best describe the dielectric as a whole [6]. When calculating the index of refraction, for example, an effective permittivity and permeability are used instead of the values from one node to another. For this reason, the wavelength must have the same approximate value as the width of the PC.

3.2.2 Transverse electric vs. transverse magnetic wave

A plane wave incident on some interface is constructed of both an E-field and H-field, which are perpendicular to each other. However, boundary conditions require that the tangential components of both fields must be continuous across the interface. Therefore E_z, E_y, H_z, H_y must be continuous at x=0, the interface. The requirements for these boundary conditions are discussed in another section. Although the wave has both an E-field and a H-field, the reflectance and transmission solutions are much easier to determine if the incident wave is broken into its perpendicular and parallel components. The perpendicular component is called a s-wave or transverse electric wave. The parallel component is known as the p wave or transverse magnetic component [18]. A transverse wave's component, electric, magnetic, etc, is perpendicular to the plane of incidence [19]. During this report only the TE aspect is investigated. The fact that the electric wave is

perpendicular to the direction of wave propagation is important because it also means that the electric field vector is parallel to the incident face of the glass slab.

3.2.3 Fresnel diffraction vs. fraunhofer diffraction

The Fresnel number (F) is a unitless parameter that helps to define what type of diffraction pattern is to be expected. F is defined as,

$$F = \frac{a^2}{\lambda L}, \quad (3.2.3.1)$$

where "a" is the aperture radius, λ is the wavelength, and L is the distance from the source to the aperture. If $F<<1$ then a Fraunhofer diffraction will occur, and if $F \geq 1$ than Fresnel diffraction will occur.

Fraunhofer diffraction is far-field diffraction, also known as parallel-beam diffraction, in which the only dependent factor is the angle from the aperture at which the location image is viewed. Fresnel diffraction is a near field diffraction and the incoming waves cannot be considered collimated waves.

3.2 FEMLAB

FEMLAB is a finite element method, multi-physics modeling software that allows the user to investigate physical results of simulations defined by partial differential equations (PDE). There are multiple uses for FEMLAB, as the software has different applications,

including acoustics, diffusion, electromagnetics, fluid dynamics, heat transfer, structural mechanics, PDE modes, and an electromagnetics module. The user must specify the area of interest when beginning the simulation setup. Although FEMLAB has the ability to run all of the modes mentioned above in 2-D and 3-D, it is only capable of running the diffusion, heat transfer, and PDE modes in 1-D.

3.2.1 FEMLAB's computational method compared to more popular methods

There are many numerical methods that can be used for analyzing a system characterized by a partial differential equation. Two main methods will be introduced in this section; the more commonly used finite difference time domain (FDTD) method and the finite element method (FEM), which FEMLAB uses.

The FDTD method is a numerical method that helps to solve PDE's. This method solves Maxwell's equations in the time domain and uses the descritization of the total spatial and temporal coordinates during numerical calculation. Although a meshing technique is used in this method, the mesh is used to help define properties, such as ε, μ, and σ, within the computational domain, which specifies the geometry region(s) over which the simulation will occur. Also, in FDTD a source must be identified instead of specifying boundary conditions to invoke an incident wave.

The FDTD method uses the relationship between the electric and magnetic fields to determine the solution, and because of this, FDTD is used specifically for electrodynamics problems. The solutions are determined in a leap-frog manner where the

solution of the electric field at some time t will be used to solve for the magnetic field at some time t'=t+dt. Also, since this is a time domain method, a large range of frequencies can be inspected within the same run.

The FEM is a numerical method used in electrical field theory, fluids, structural mechanics etc., to help solve PDE's. The system is broken down into a mesh and the PDE is investigated at nodes in the mesh [20]. The size of the meshing will determine how many nodes will lie within the geometry. Looking at a simple geometry, the original and meshed parts can be seen and compared below.

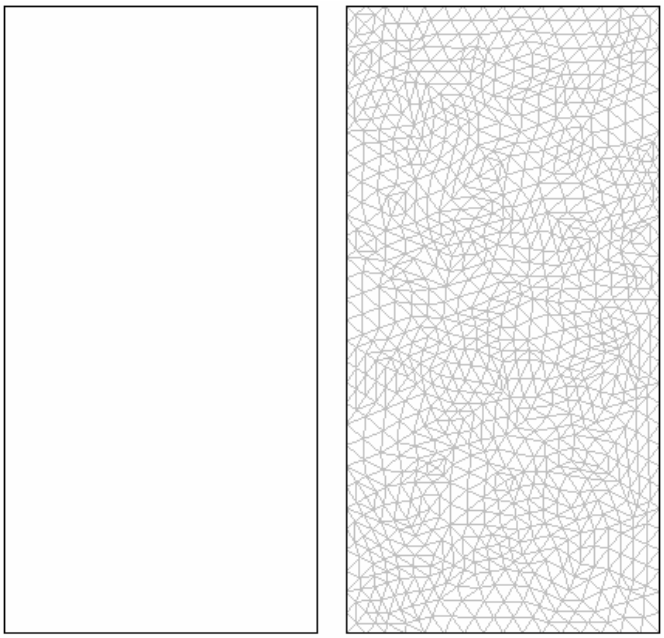

Figure 11: Original and meshed geometry comparison

This method can be done analytically, which will give more precise answers and will involve using the solution of the PDE at one node to determine the solution for the PDE at the following node. The other option is to use a computer to obtain a numerical

solution. If a FEM program is used, such as FEMLAB, approximated answers will only be given at discrete locations on the mesh. For the simulation described later in this paper, FEMLAB solves Maxwell's equations for discrete locations within the geometry.

3.2.2 Why FEMLAB

After reading through some of the available literature, I realized that not many articles looked at the reflectance properties of the LHM. Most reports, such as Pendry et al.'s mentioned in the "Literature Review" section, set the material's properties to be lossless so that the transmissive qualities of the material could be investigated [9]. Due to the field of work I am involved in, I wanted to see what the reflectance values for a wavelength in the near infrared (NIR) or mid-wave (MWIR) infrared region would look like when an incidence angle of theta is used. Since I am unable to create this scenario within a laboratory setting, I used the software that was available to me. There are multiple types of software that can be used to create such simulations, as discussed later, but I had the most access to FEMLAB.

3.2.3 Deriving single equation for FEMLAB

One of the first steps in setting up a model in the Electromagnetics Module is to determine what kind of wave you have, TE, TM, etc. After the type of model is chosen and the geometry is created, the PDE that is to be solved can be found under Physics>Subdomain. For an "In Plane TE Wave," as FEMLAB defines it, the equation to be solved is $\nabla \times (\mu_r^{-1} \nabla \times E_z) - (\varepsilon_r - i\sigma/\omega\varepsilon_0) k_0^2 E_z = 0$, where $\varepsilon_r = n^2$ and k_0 is the

wave vector. The following derivation shows the steps necessary to start with Maxwell's equations, the starting point for all equations used in the Electromagnetics Module, and end with the equation used in the FEMLAB solution described throughout this report [21].

Revisiting Maxwell's equations, Maxwell-Ampere's and Faraday's laws will be the first step in this derivation.

$$\nabla \times \vec{H} = \frac{\partial \vec{D}}{\partial t} + \vec{J}, \tag{3.2.3.1}$$

$$\nabla \times \vec{E} = -\frac{\partial \vec{B}}{\partial t}. \tag{3.2.3.2}$$

Noting that $\vec{J} = \sigma \vec{E}$, $\vec{D} = \varepsilon \vec{E}$ and $\vec{B} = \mu \vec{H}$ allows the equations to be rewritten as

$$\nabla \times \vec{H} = \tilde{\varepsilon} \frac{\partial \vec{D}}{\partial t} + \sigma \vec{E}, \tag{3.2.3.3}$$

$$\nabla \times \vec{E} = -\mu \frac{\partial \vec{H}}{\partial t}. \tag{3.2.3.4}$$

In the rewritten Maxwell-Ampere equation, $\tilde{\varepsilon}$, the complex permittivity, is defined as $\tilde{\varepsilon} = \varepsilon' - i\varepsilon'' = \varepsilon - i\sigma/\omega$. The time harmonic form of $\vec{E}$ and $\vec{H}$, which is $\vec{E}(x, y, z, t) = E(x, y, z)e^{i\omega t}$ and $\vec{H}(x, y, z, t) = H(x, y, z)e^{i\omega t}$, can be combined with equations (3.2.3.3) and (3.2.3.4) above to create the equation similar to the one used in FEMLAB.

$$\begin{aligned} \nabla \times (\mu_r^{-1} \nabla \times \vec{E}) - \omega^2 \tilde{\varepsilon} \vec{E} = 0, \\ \nabla \times (\tilde{\varepsilon}^{-1} \nabla \times \vec{H}) - \omega^2 \mu \vec{H} = 0. \end{aligned} \tag{3.2.3.5}$$

Since the presented model's glass slab lies within the x-y plane, the electric field is pointed in the z-direction. The governing equation then becomes

$$\nabla \times (\mu_r^{-1} \nabla \times E_z) - (\varepsilon_r - i\sigma/\omega\varepsilon_0) k_0^2 E_z = 0. \qquad (3.2.3.6)$$

3.2.4 Perfectly matched layers

A perfectly matched layer (PML) is a method for solving unbounded electromagnetic problems using the finite element method. The PML formulation can be derived from Maxwell's equations by introducing a complex-valued coordinate transformation. A PML is designed to surround the geometry model and absorb incoming electromagnetic waves without causing reflections. The material's anisotropic permittivity and permeability must match the permittivity and permeability of the physical medium outside the PML in such a way that no reflections occur.

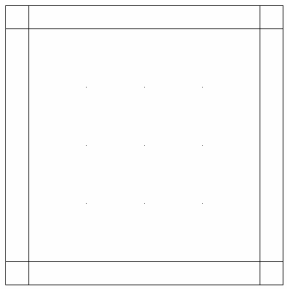

Figure 12: PML used in FEMLAB runs

The PML used in these FEMLAB runs consisted of four rectangles as shown in Figure 12 above. Boundary conditions, explained in a later section, include an electric field propagating in the x-direction moving from left to right beginning at the left outer face of

the PML. For the geometry in FEMLAB, the electromagnetic wave makes an angle φ=90° with the y-axis. Proof that no reflections occur while the wave is propagating through the PML, for the general case where the angle is some arbitrary φ, is derived in Appendix A.

The first step to creating a PML in FEMLAB, is to implement a sub domain with an absorbing layer and anisotropic material parameters. The new sub domains' defining equations include $\mu = \mu_0 \mu_r L$ and $\varepsilon = \varepsilon_0 \varepsilon_r L$, where L is a diagonal two rank tensor. L's components allow the user to create a PML that absorbs waves traveling in a set direction. Values for L below define a PML attenuating a wave traveling in the x-direction through the parameters s_x, s_y, and s_z, which are complex-valued coordinate scaling parameters.

$$L_{xx} = \frac{s_y s_z}{s_x}, \quad L_{xx} = \frac{s_z s_x}{s_y}, \quad L_{xx} = \frac{s_x s_y}{s_z}, \tag{3.2.4.1}$$

where the s-values are defined as s_x=a-bi=1-i for this model, and s_y= s_z=1 because the wave is traveling in the x-direction.

The wave traveling some distance Δx through the PML will experience some loss in electric field intensity due to the presence of evanescent waves. The field value can be calculated using the equation $E_0 = |E_{0z}| e^{-bk_0 \Delta x}$, where b is the imaginary s_x component, k_0 is the wave number, and Δx is the PML's thickness in the direction the wave is traveling.

To ensure a high enough electric field propagates through the PML, the user must ensure that the PML width is of the same order of magnitude as the wavelength being used [22].

During the FEMLAB run, the solution for the electric field in the z direction is solved.

3.3 Fresnel's Equations

Fresnel's equations are fundamental equations used to numerically define the reflectance and transmittance properties of an interface. These equations are used to determine both the FEMLAB and Fabry-Perot results of a glass slab.

First the traditional approach to the incident, reflected, and transmitted values will be used to fully explain the Fresnel equation concepts. The first step is to design a diagram, Figure 13, to explain the location of the interface and the direction of wave motion:

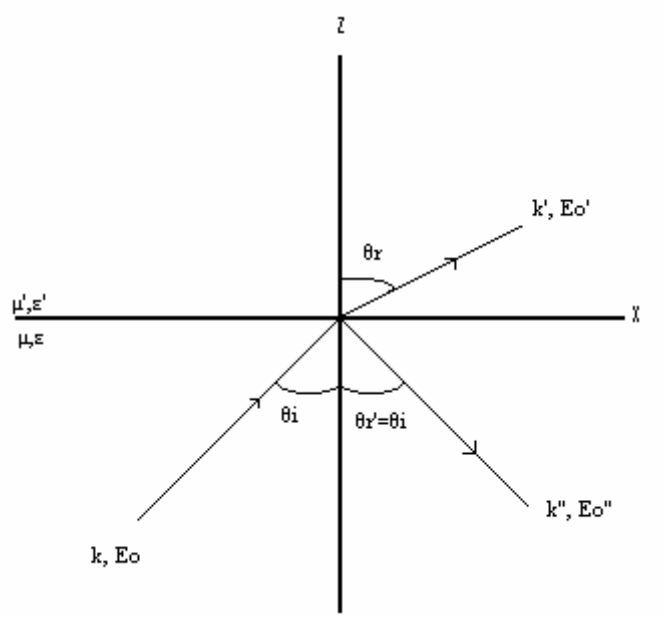

Figure 13: Diagram depicting location of interface and direction of wave motion

There are three parts to this diagram:

- Incident wave (k)

$$\vec{E} = \vec{E}_0 e^{(\vec{k}\cdot\vec{r} - i\omega t)}, \qquad \vec{B} = \frac{n}{c}\vec{k} \times \vec{E}. \tag{3.3.1}$$

- Refracted wave (k')

$$\vec{E} = \vec{E}_0^{'} e^{(\vec{k}'\cdot\vec{r} - i\omega t)}, \qquad \vec{B}' = \frac{n'}{c}\vec{k}' \times \vec{E}'. \tag{3.3.2}$$

- Reflected wave (k'')

$$\vec{E}'' = \vec{E}_0^{''} e^{(\vec{k}''\cdot\vec{r} - i\omega t)}, \qquad \vec{B}'' = \frac{n}{c}\vec{k}'' \times \vec{E}''. \tag{3.3.3}$$

Looking at the boundary conditions for this system at z=0 gives the relationship $(\vec{k} \cdot \vec{x})_{z=0} = (\vec{k}' \cdot \vec{x})_{z=0} = (\vec{k}'' \cdot \vec{x})_{z=0}$. This condition must be fulfilled and therefore, the wave vectors must lie within the plane $k \sin\theta_i = k' \sin\theta_r = k'' \sin\theta_{r'}$. Other boundary conditions that must be fulfilled at z=0 are that the normal components of $\vec{D}$ and $\vec{B}$ are continuous and the tangential components of $\vec{E}$ and $\vec{H}$ are continuous.

Applying these conditions to equations (3.3.1)-(3.3.3) the defining equations become

$$\begin{aligned} \vec{E}_0 + \vec{E}_0'' &= \vec{E}_0', \\ \vec{B}_0 + \vec{B}_0'' &= \vec{B}_0'. \end{aligned} \tag{3.3.4}$$

For this case, we are interested in the polarization of $\vec{E}$ being perpendicular to the plane of incidence, which is the plane defined by **k** and **n** [22]. This type of wave is called a s-wave or Transverse Electric (TE) wave. Figure 14 gives the diagram for a TE wave [22].

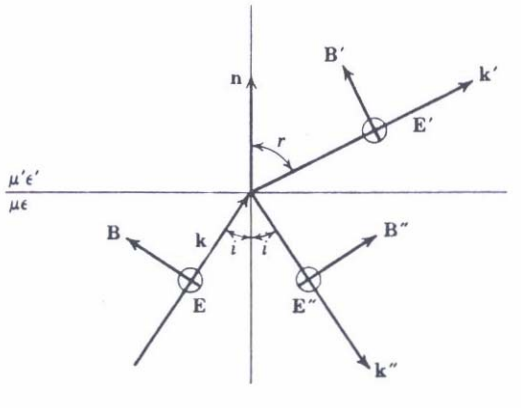

Figure 14: Diagram of electric field perpendicular to plane of incidence

Also noting the laws of reflection and refraction [24] and referring to the figure above the equations above become

$$\begin{aligned} &E_0 + E_0^{''} - E_0^{'} = 0, \\ &n(E_0 - E_0^{''})\cos\theta_i - n' E_0^{'} \cos\theta_r = 0. \end{aligned} \tag{3.3.5}$$

Assuming the value for E_0 is known, there are now two equations and two unknowns. The next step is to determine the reflected and transmitted amplitudes. These ratios are known as Fresnel's equations for polarization perpendicular to the plane of incidence.

$$\text{Transmitted amplitude: } \frac{E_0^{'}}{E_0} = \frac{2n\cos\theta_i}{n\cos\theta_i + n'\cos\theta_r}, \tag{3.3.6}$$

$$\text{Reflected amplitude: } \frac{E_0^{''}}{E_0} = \frac{n\cos\theta_i - n'\cos\theta_r}{n\cos\theta_i + n'\cos\theta_r}. \tag{3.3.7}$$

The reflected and transmitted values can be found through the following equations

$$T = \left|\frac{E_0^{'}}{E_0}\right|^2 \text{ and } R = \left|\frac{E_0^{''}}{E_0}\right|^2. \tag{3.3.8}$$

The above equations are for a general angle of incidence, however for a normal angle of incidence the reflected and transmitted equations can be reduced to:

$$\frac{E_0^{'}}{E_0} = \frac{2n}{n+n'}, \tag{3.3.9}$$

$$\frac{E_0^{''}}{E_0} = \frac{n-n'}{n+n'}. \tag{3.3.10}$$

As mentioned earlier, the wave has been separated into two components; one where the electric field is perpendicular to the plane of incidence and one where it is parallel to the plane of incidence. The next step is to look at the case where the electric field is parallel to the plane of incidence and therefore the magnetic field is perpendicular to the plane of incidence. Figure 15 is a diagram of a Transverse Magnetic (TM) wave [22].

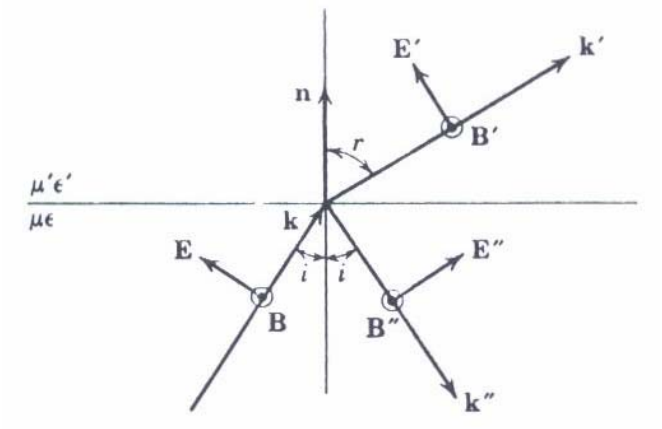

Figure 15: Diagram of electric field parallel to plane of incidence

Returning to the original boundary conditions in (3.3.4), only the second equation is not applicable to this scenario.

$$\begin{aligned} nE_0 + nE_0^{"} &= n'E_0^{'}, \\ E_0\cos\theta_i - E_0^{"}\cos\theta_i &= E_0^{'}\cos\theta_r . \end{aligned} \tag{3.3.14}$$

Solving for the transmission ($E_0^{'}$) and reflection ($E_0^{"}$) coefficients gives

$$\text{Transmitted amplitude: } \frac{E_0^{'}}{E_0} = \frac{2n\cos\theta_i}{n\cos\theta_r + n'\cos\theta_i}, \tag{3.3.15}$$

$$\text{Reflected amplitude: } \frac{E_0^{"}}{E_0} = \frac{n'\cos\theta_i - n\cos\theta_r}{n\cos\theta_t + n'\cos\theta_i}. \tag{3.3.16}$$

The reflected and transmitted values can be found through the following equations:

$$T = \left|\frac{E_0^{'}}{E_0}\right|^2 \text{ and } R = \left|\frac{E_0^{"}}{E_0}\right|^2 .$$

The above are the equations for a general angle of incidence, however for a normal angle of incidence equations (3.3.8) and (3.3.9) can be reduced to

$$\frac{E_0^{'}}{E_0} = \frac{2n}{n+n'}, \tag{3.3.17}$$

$$\frac{E_0^{"}}{E_0} = \frac{n'-n}{n+n'}. \tag{3.3.18}$$

3.4 Fabry-Perot Equations

Although the actual Fresnel equations are extremely important and are a necessity for this report, there are other ways to derive and use their results. In some cases the derivation is not as simple as involving a single reflection of an interface. For the geometry used in this report, multiple reflections on both sides of the glass slab must be included in the calculation to properly calculate the reflection and transmission coefficients. See Figure 17, in the next section, for diagram on multiple reflectances.

3.4.1 Electrodynamic approach

Assuming a glass slab is surrounded by another medium, such as air, the first step in solving for the reflection and transmission coefficients is to define the refractive indices of the materials,

$$n = \begin{cases} n_1, & x < 0 \\ n_2, & 0 < x < d \\ n_3, & d < x \end{cases} . \qquad (3.4.1.1)$$

Assuming the plane of incidence is the xz plane, I am able to write the electric field (plane wave solution) as [18]

$$E(x)e^{i(\omega t - \beta z)},$$

where β is the z-component of the wave vector k.

Defining constants, with the plane wave incident from the left, E(x) can be written as:

$$E(x) = \begin{cases} Ae^{-ik_{1x}x} + Be^{ik_{1x}x}, & x < 0 \\ Ce^{-ik_{2x}x} + De^{ik_{2x}x}, & 0 < x < d \\ Fe^{-ik_{3x}(x-d)}, & d < x \end{cases} . \quad (3.4.1.2)$$

Note that k_{ix} is the wave vector in the x-direction and i denotes which section (1, 2, 3) the wave is traveling in.

$$k_{ix} = ((\frac{n_i \omega}{c})^2 - \beta^2)^{1/2} = (\frac{\omega}{c}) n_i \cos\theta_i , \quad (3.4.1.3)$$

where θ_i is the angle of incidence from the x-axis. Another important note is that A is the amplitude of incident wave, B is the amplitude of reflected wave, and F is the amplitude of transmitted wave.

Boundary conditions require that the tangential component of the E-field and H-field (remember $H = B/\mu$) must be continuous across each interface. For an s-polarized (also known as TE) wave, E_y and H_z must be continuous. Applying these boundary conditions and noting that $H_z = \frac{i}{\omega\mu}(\frac{\partial E}{\partial x})$, where E(x) has been defined earlier,

$$H_z = \begin{cases} \frac{k_{1x}}{\omega\mu}(Ae^{-ik_{1x}x} + Be^{ik_{1x}x}), & x < 0 \\ \frac{k_{2x}}{\omega\mu}(Ce^{-ik_{2x}x} - De^{ik_{2x}x}), & 0 < x < d \\ \frac{k_{3x}}{\omega\mu} Fe^{-ik_{3x}(x-d)}, & d < x \end{cases} . \quad (3.4.1.4)$$

Imposing the boundary conditions at x=0, d gives the following equations

$$
\begin{aligned}
&A + B = C + D,\\
&k_{1x}(A - B) = k_{2x}(C - D),\\
&Ce^{-ik_{2x}d} + De^{ik_{2x}d} = F,\\
&k_{2x}(Ce^{-ik_{2x}d} - De^{ik_{2x}d}) = k_{3x}F.
\end{aligned}
\tag{3.4.1.5}
$$

Now solving for B, C, D, and F

$$
\begin{aligned}
F &= A\frac{4k_{1x}k_{2x}e^{-ik_{2x}d}}{(k_{1x}+k_{2x})(k_{2x}+k_{3x})+(k_{1x}-k_{2x})(k_{2x}-k_{3x})e^{-ik_{2x}d}},\\
B &= A\frac{(k_{1x}+k_{2x})(k_{2x}+k_{3x})+(k_{1x}+k_{2x})(k_{2x}-k_{3x})e^{-ik_{2x}d}}{(k_{1x}+k_{2x})(k_{2x}+k_{3x})+(k_{1x}-k_{2x})(k_{2x}-k_{3x})e^{-ik_{2x}d}},\\
C &= \frac{1}{2}F(1+\frac{k_{3x}}{k_{2x}})e^{ik_{2x}d},\\
D &= \frac{1}{2}F(1-\frac{k_{3x}}{k_{2x}})e^{-ik_{2x}d}.
\end{aligned}
\tag{3.4.1.6}
$$

Recalling $k_{ix} = (\frac{\omega}{c})n_i\cos\theta_i$ and writing the Fresnel reflection and transmission amplitude coefficients for a dielectric interface and s-polarization then I can write:

$$
\begin{aligned}
r_{12} &= \frac{k_{1x}-k_{2x}}{k_{1x}+k_{2x}},\\
r_{23} &= \frac{k_{2x}-k_{3x}}{k_{2x}+k_{3x}},
\end{aligned}
\tag{3.4.1.7}
$$

$$
\begin{aligned}
t_{12} &= \frac{2k_{1x}}{k_{1x}+k_{2x}},\\
\text{and}\quad t_{23} &= \frac{2k_{2x}}{k_{2x}+k_{3x}}.
\end{aligned}
\tag{3.4.1.8}
$$

I also know that the reflection amplitude coefficient is represented as the ratio of the reflected wave amplitude, B, to that of the incident wave amplitude, A and the

transmitted amplitude coefficient is the ratio of the transmitted wave amplitude, F, to that of the incident wave, A;

$$r = \frac{B}{A} \text{ and } t = \frac{F}{A}.$$

As the wave travels through medium 2 a phase change will occur of

$$\phi = k_{2d} d = \frac{2\pi d}{\lambda} n_2 \cos\theta_2 . \tag{3.4.1.9}$$

Incorporating this phase change into the equations for the reflection and transmission amplitude coefficients

$$\begin{aligned} r &= \frac{B}{A} = \frac{r_{12} + r_{23} e^{-2i\phi}}{1 + r_{12} r_{23} e^{-2i\phi}}, \\ t &= \frac{F}{A} = \frac{t_{12} t_{23} e^{-i\phi}}{1 + r_{12} r_{23} e^{-2i\phi}}. \end{aligned} \tag{3.4.1.10}$$

3.4.2 Airy's formulation

This theory is used in the case of multiple beam interference and uses the ray method by tracing and following the path of the wave as it interacts with a dielectric [18]. In this case the ray diagram would appear as shown below.

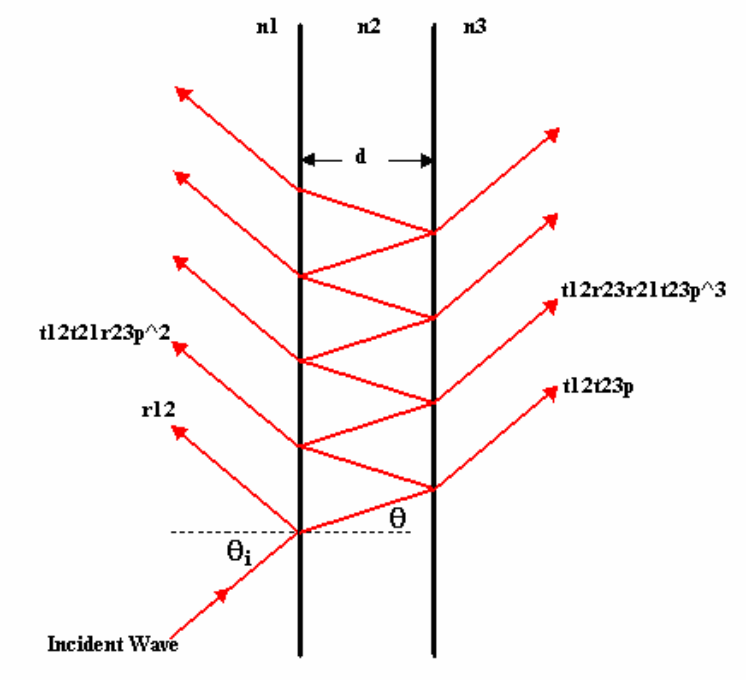

Figure 16: Diagram showing multiple reflections caused by a finite slab

In the diagram above $p = e^{-i\phi}$ and takes into account the phase changes. As the incident wave interacts with the second medium, part of the wave will be reflected (r12) and part of it will be transmitted (t12). Part t12 will then interact with the interface between the second and third medium where part of t12 will be reflected (t12r23) and part will be transmitted (t12t23), etc.

For simplicity, the incident wave's value is assumed to be one, and the next step in solving the overall reflection and transmission amplitude coefficients is to sum the terms on the left side of n_2 (the reflected waves) and then sum the terms on the right (the transmitted terms). The following equations reveal these steps.

$$
\begin{aligned}
r &= r_{12} + t_{12}t_{21}r_{23}e^{-2i\phi} + t_{12}t_{21}r_{23}r_{21}r_{23}e^{-4i\phi} + \ldots \\
&= r_{12} + \frac{t_{12}t_{21}r_{23}e^{-2i\phi}}{1 + r_{12}r_{23}e^{-2i\phi}} \\
&= \frac{r_{12} + r_{23}e^{-2i\phi}}{1 + r_{12}r_{23}e^{-2i\phi}},
\end{aligned}
\tag{3.4.2.1}
$$

$$
\begin{aligned}
t &= t_{12}t_{23}r_{23}e^{-i\phi}(1 + r_{23}r_{21}e^{-2i\phi} + (r_{23}r_{21}e^{-2i\phi}) + \ldots \\
&= \frac{t_{12}t_{23}e^{-i\phi}}{1 - r_{21}r_{23}e^{-2i\phi}} \\
&= \frac{t_{12}t_{23}e^{-i\phi}}{1 + r_{21}r_{23}e^{-2i\phi}}.
\end{aligned}
\tag{3.4.2.2}
$$

Note that the phase change is defined as

$$
\phi = \frac{2\pi}{\lambda} n_2 d \cos\theta_2 . \tag{3.4.2.3}
$$

The coefficients r_{ij} and t_{ij} are determined using the equations

$$
\begin{aligned}
r_{ij} &= \frac{k_{ix} - k_{jx}}{k_{ix} + k_{jx}}, \\
t_{ij} &= \frac{2k_{ix}}{k_{ix} + k_{jx}}.
\end{aligned}
\tag{3.4.2.4}
$$

which are just generalized versions of the equations that were solved for in the previous section.

Both methods of derivation require an understanding of the Fresnel equations, and require their solutions to be integrated into the equations given above. Both methods also result in the same solution for the reflection and transmission coefficients.

3.4.3 Preparing equations for LHM

The Fresnel equations above are appropriate for a positive index of refraction. However, for the case of a left-handed metamaterial the refractive index needs to be represented using its relationship to the material's wave impedance, Z [2].

$Z = \sqrt{\frac{\mu}{\varepsilon}}$, where Z>0 for all cases, including those where ε, μ<0.
$n = \pm\sqrt{\mu\varepsilon}.$

Going back to the solutions for Fresnel's equations and noting that

$$\begin{aligned} &E_0 + E_0^{"} = E_0^{'}, \\ &\frac{1}{Z_1}\hat{k}\cdot\hat{n}\vec{E} + \frac{1}{Z_1}\hat{k}^{"}\cdot\hat{n}\vec{E}^{"} = \frac{1}{Z_2}\hat{k}^{'}\cdot\hat{n}\vec{E}^{'}. \end{aligned} \tag{3.4.11}$$

Using these equations, the Fresnel equations solutions can be rewritten, for all angles of incidence, as

$$E_0^{'} = \frac{2Z_2\cos\theta_i}{Z_2\cos\theta_i + Z_2\cos\theta_r}E_0 \Rightarrow \left|\frac{E_0^{'}}{E_0}\right|^2 = T, \tag{3.4.12}$$

$$E_0^{"} = \frac{Z_2\cos\theta_i - Z_1\cos\theta_r}{Z_2\cos\theta_i + Z_2\cos\theta_r}E_0 \Rightarrow \left|\frac{E_0^{"}}{E_0}\right|^2 = R. \tag{3.4.13}$$

According to Veselago, the Fresnel equation, with the refractive index, cannot be properly applied to the case of a LHM. For the situation where a LHM is used, the wave impedance of the material must be included in Fresnel's equation. Since the Fabry-Perot equation's base is the Fresnel equation, the wave impedance must also be included to properly represent an LHM's physical properties.

Looking back to (3.4.1.11),

$$r = \frac{\{r_{12}\} + r_{23}e^{-2i\phi}}{1 + r_{12}r_{23}e^{-2i\phi}}, \tag{3.4.14}$$

$$r_{ij} = \frac{k_{ix} - k_{jx}}{k_{ix} + k_{jx}},$$

$$k_{ix} = (\frac{\omega}{c})n_i \cos\theta_i .$$

Please note that (3.4.14) is the simplified version of the Fabry-Perot equation, and when expanded reveals the wave impedance. The section within the curly brackets of the Fabry-Perot reflectance equation, located above, is the definition of r_{12}. r_{12} is the only part of the equation that can be compared to the Fresnel equation because the Fresnel equation only takes into account one interface, while the Fabry-Perot takes into account multiple reflections caused by two interfaces.

The result found using the wave impedance in this first section, r_{12}, is the same as found in the Fresnel equations.

4 MODELING PROCESS

A 2-D glass slab was created and was given a negative value for the index of refraction. This slab has been enclosed within a boundary of perfectly matched layers, as shown in Figure 17 below. The entire geometry is made of six parts. R1 is the glass slab, R2-R5 are the PML, as discussed in an earlier section, and R6 is a rectangle whose sub domain properties are those of air. Table 2 gives a quick overview of the physical properties used to create the geometry used during the LHM FEMLAB runs.

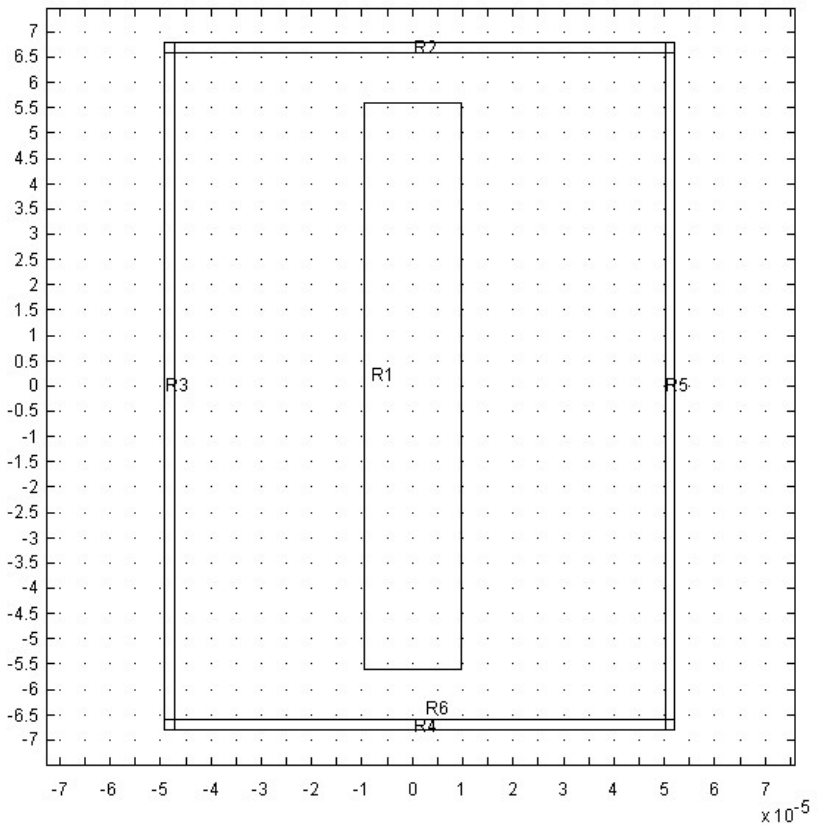

Figure 17: FEMLAB geometry input

Slab width	19 μm
Slab Height	112 μm
Slab ε	-3
Slab μ	-1
Wavelength	4 μm

Table 2: Geometry parameters

Once the FEMLAB program has been opened, a new 2-D file can be made by choosing 2-D>Electromagnetics Module>In-plane waves>TE waves, which will open an empty grided screen. Before creating the geometry, the grid size needs to be changed by clicking "Options>Axes/Grid Settings." The new x minimum and maximum should be set as shown below and the grid size, in both the x and y direction should be changed to $1e^{-6}$ by clicking on the grid tab and unchecking the auto box, an example of these settings is shown in Figure 18. This allows the user to create the geometry in microns.

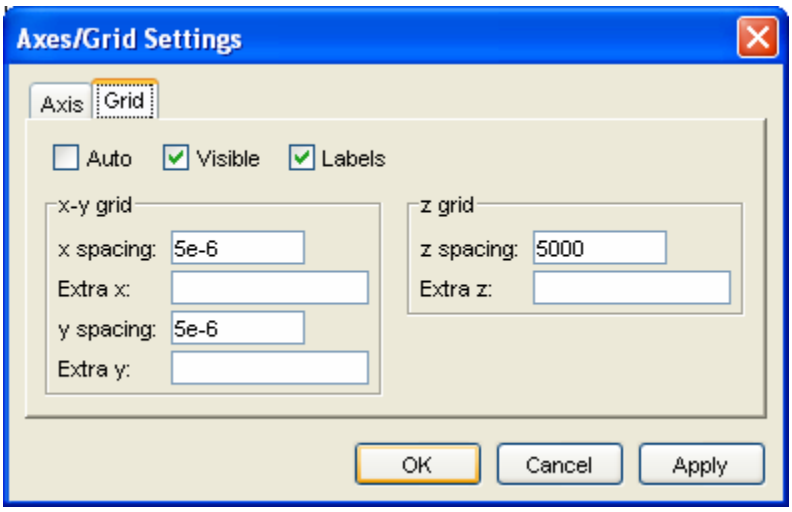

Figure 18: Geometry axes settings

As mentioned before, the PML's sub domain will be defined by a rank two tensor, L, whose directional components will be set for a wave traveling in the x-direction through the values of s_x, s_y, and s_z. It is necessary to define the constants a, b, s_x, s_y, s_z, L_{xx}, L_{yy}, and L_{zz} to continue the simulation. First step is to define a and b by choosing "Options>Constants." Second is to define L_{xx}, L_{yy}, and L_{zz} through "Options>>Scalar Expressions," and in order to define s_x, s_y, and s_z "Options>Expressions>Sub domain expressions" must be clicked. Values for all three settings are shown below in Figures 19 and 20 and Table 3.

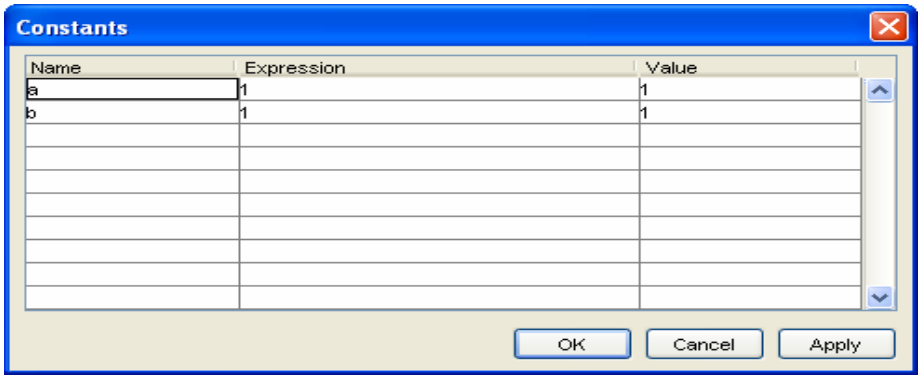

Figure 19: Values for constants a and b

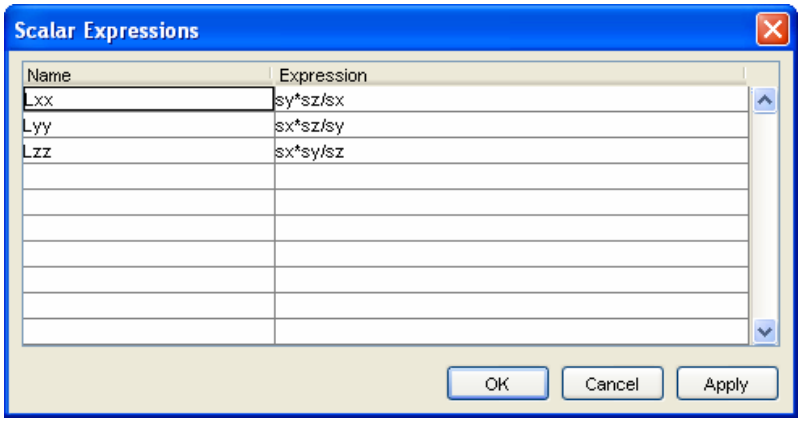

Figure 20: Values for scalar expressions L_{xx}, L_{yy}, and L_{zz}

Sub domain	1,3,7,9	2,8	4,6
s_x	a-b*i	a-b*i	1
s_y	a-b*i	1	a-b*i
s_z	1	1	1

Table 3: Sub domain settings for s_x, s_y, s_z

In this simulation, a wavelength matching the mid-wave infrared region will be used. To set the wavelength value click "Physics>Scalar Variables" and change the frequency to 3e8/4e-6. Remember that the frequency of a wave is defined as $\upsilon = c/\lambda$, where c is the speed of light in m/s.

After defining all the constants, the next step is to build the actual geometry parts using the dimension shown in Table 4 below. All positions, except R1, are given from their lower left corner.

	R1	R2	R3	R4	R5	R6
Width	19	101	2	101	2	57
Height	112	2	136	2	136	57
X position	Centered at 0	-49	-49	-49	50	-47
Y position	Centered at 0	66	-68	-68	-68	-66

Table 4: Dimensions and locations of geometry pieces in micrometers

Once the geometry has been built, the next step is to define the sub domain settings through "Physics>Sub domains." Highlight multiple sub domains by holding the ctrl key during the selection process. A material's properties can either be defined by its relative

permittivity, ε_r, and relative permeability, μ_r, or by refractive index, n. Each sub domain's properties are defined below.

Sub domain	**1-4, 6, 8-10**	**5**	**7**
ε_r	L_{zz}	1	
μ_r	anisotropic, L_{xx} 0 0 L_{yy}	1	
n			1.8

Table 5: Sub domain settings as found in "Physics>Sub domain"

"Physics>Boundary Settings" allows the boundary conditions of the geometry to be defined. Although there are 28 boundaries in this geometry, only the exterior boundaries are being defined. Figures 21 and 22 give the boundary settings for boundaries 1, 3, 5, and 26-28. Please note that the equations shown in Figures 21 and 22 are boundary condition equations and are not the PDE FEMLAB is solving. These boundary condition equations are dependent upon the type of condition the user chooses.

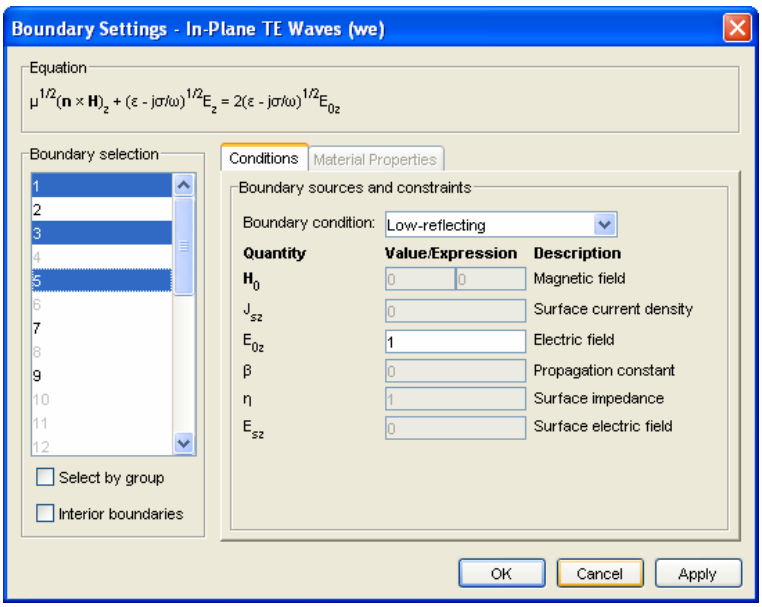

Figure 21: Boundary settings for boundaries 1, 3, and 5

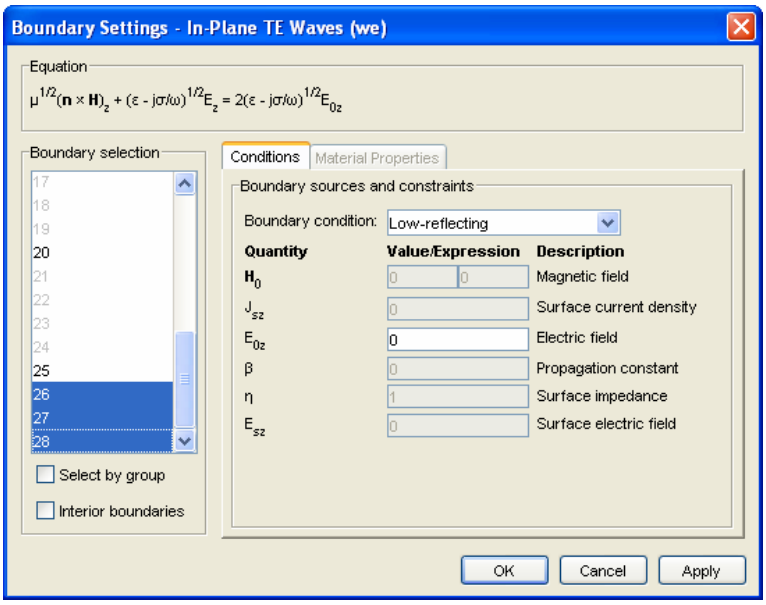

Figure 22: Boundary settings for boundaries 26-28

For boundaries 7, 9, 14, 20, 25, the top and bottom boundaries, the boundary conditions need to be set as a perfect magnetic conductor. The magnetic field of the incoming wave

is normal to these boundaries since the wave is propagating in the x-direction. This direction of motion is why these boundaries must be set as perfect magnetic conductors.

FEMLAB's automatic setting for the geometry mesh is 1/15 of the grid's unit value. For this simulation the automatic mesh setting will be 1/15 of a micrometer. However, this mesh size is too large for the simulation and must be change. There are two ways altering the mesh size. The mesh setting can be found under "Mesh> mesh parameters" and then entering the desired value under "Maximum element size" and entering the value $1*10^{-6}$ which gives 59512 elements. The other way is to simply use the "Refine Mesh" button along the top of FEMLAB. Pushing this button three times will also increase the mesh elements to approximately the same size. A "before and after" mesh view is given in the figure below.

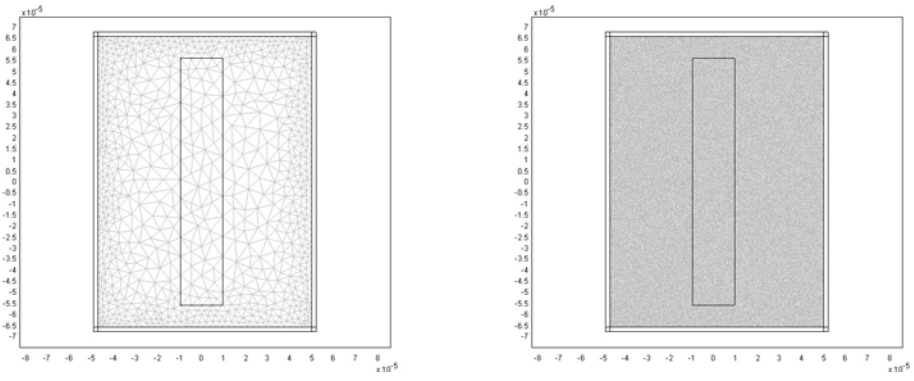

Figure 23: Original 2350 element mesh (left) and refined 59512 element mesh (right)

In order to only visualize the resulting reflected and transmitted waves, the incident wave needs to be suppressed. The first step in this is to suppress the PML sub domains through "Options>Suppress> Suppress sub domains" and choosing sub domains 1-4, 6, 8-10.

Next go to "Post processing> Plot parameters>Surface tab" and enter $E_z - e^{i*phase}e^{-(x+X1)ik0\_we)}e^{(X2)k0\_we}$ in the expression slot. The first component of this equation, E_z, represents the total electric field; incident, reflected, and transmitted. The second part, which is broken down into three exponential subparts, represents the plane wave. The first exponential subpart allows FEMLAB to vary the phase of the solution during the animation process and to correctly visualize the animation through the variation of the wave's phase. The second term expresses the relative phase change of the plane wave as it travels in the x-direction. The third subpart represents the damping of the wave as it propagates through the defined PML before entering the air domain

[21]. In both the second and third part of the exponential function, k0_we represents the wave number within air. X1 in the equation represents the position where the wave begins in the geometry. In the geometry used, the wave moves from left to right beginning at the outer edge of the PML; X1= $-4.9*10^{-5}$. X2 is the thickness of the PML in the x-direction; X2=$2*10^{-6}$. Using this equation during visualization, one can determine the value of the reflected electric field.

5 RESULTS

Three types of studies, one explaining and two verifying the results, will be discussed in the following sections. First, FEMLAB's visual solution and the law of refraction will be used to verify the software's ability to properly simulate a negative refraction. Second, the reflectivity of the glass slab will be inspected. During this process, the theoretical values will be calculated by inserting ε and μ values, same values used during the FEMLAB runs, into the Fabry-Perot equations to obtain the reflectance value. Also during these calculations, the E_z values given by FEMLAB, determined from the visualization of the equation $E_z - e^{i*phase}e^{-(x+X1)ik0\_we)}e^{(X2)k0\_we}$, will be used to determine the reflectance value using the Fresnel equations. Comparing the two values will reveal FEMLAB's ability to accurately simulate the physical properties of an LHM. Third, Veselago's theory of *n* vs. *Z* will verified.

A simple Matlab routine was written to help calculate the reflectance values. The user can simply input the necessary constant values and complete the run. This routine was used for both the theoretical and FEMLAB values calculations. The Matlab routine can be found in the appendix. The incident amplitude value is defined during the simulation setup, and in this case $E_0 = |E_{0z}|e^{-bk_0\Delta x} = 0.0432$ after the wave has propagated through the PML.

5.1 FEMLAB Solution Visualization Verification

Before beginning any calculations, FEMLAB's ability to properly visualize the solution of a wave traveling through an LHM should be verified. In order to do so, a glass slab was modeled within FEMLAB and the results of $n>0$ and $n<0$ were visually compared. As presented in an earlier section, the refracted wave's path is on the same side of the normal as the incident wave.

Incident Angle	First interface transmission angle $n>0$	First interface transmission angle $n<0$	Second interface transmission angle $n>0$
0	0	0	0
5	2.8843	-2.8843	5
10	5.7539	-5.7539	10
15	8.5939	-8.5939	15
20	11.3888	-11.3888	20
25	14.1227	-14.1227	25

Table 6: Comparison of refraction angle for $n>0$ and $n<0$

Table 6 above proves, using Snell's Law, that theoretically the transmitted wave for a LHM will travel a different path than that of a normal material. Figures 24 and 25 below show E_z for $n<0$ and $n>0$, and prove that FEMLAB does correctly visualize the transmission path for a wave traveling through an LHM.

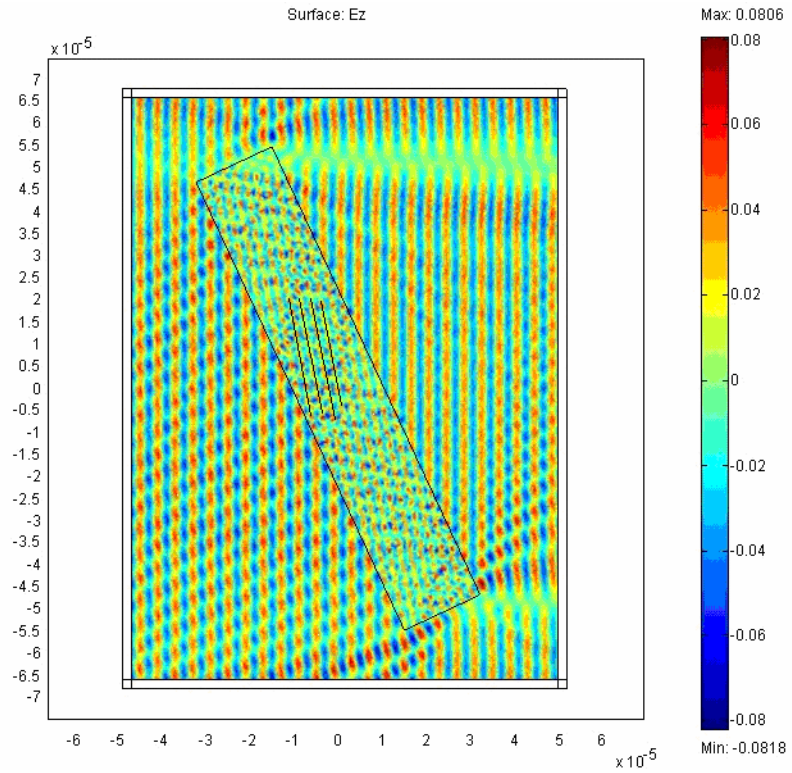

Figure 24: Refraction path for $n>0$

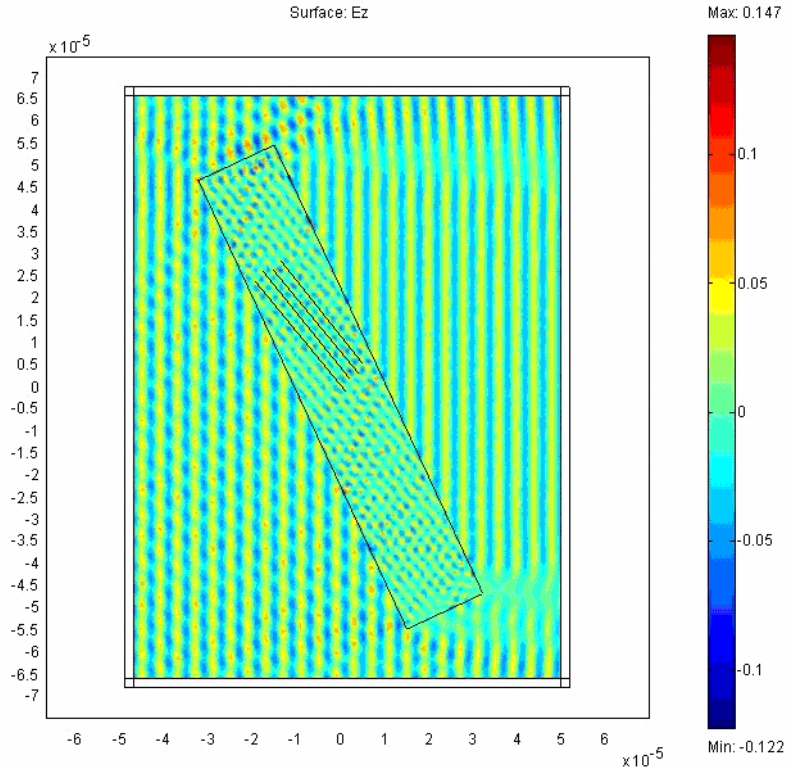

Figure 25: Refraction path for $n<0$

Lines have been added to the above figures to help the viewer follow each slab's transmission path. When comparing the images above, one can see the distinct path change between FEMLAB's visualization of $n>0$ and $n<0$. This shows the results of negative refraction.

5.2 FEMLAB Results Verification

By following the model instructions just given, a glass slab, whose physical properties include a refractive index greater than zero, was built. The reason for first creating a positive index of refraction glass slab is so that these results can be compared to those obtained through the Fabry-Perot equations. This is an important step in the modeling process, because the user wants to verify that they are obtaining correct answers from FEMLAB. Calculations will be completed using an incidence angle of zero. Once the FEMLAB values are validated, the results of the LHM will be presented.

5.2.1 Expected values

For this first case $\theta_i=0$, and therefore the above equation for the reflectivity value can easily be simplified to

$$r = \frac{r_{12} + r_{23}e^{-2i\phi}}{1 + r_{12}r_{23}e^{-2i\phi}}. \qquad (5.1.1.1)$$

Since the properties for ε_1 and μ_1 are set to those of air, $\varepsilon_1=1$ and $\mu_1=1$, and the angle of incidence is 0° the above equation can be reduced to

$$r = \frac{\frac{n_1 - n_2}{n_1 + n_2} + \frac{n_2 - n_3}{n_2 + n_3} e^{-2i\phi}}{\frac{\lambda}{2\pi} + \frac{n_1 - n_2}{n_1 + n_2} \frac{n_2 - n_3}{n_2 + n_3} e^{-2i\phi}}. \qquad (5.1.1.2)$$

For this section $\mu_2 = 1$ and $\varepsilon_2 = 3$. Therefore the reflectance coefficient is $|r|^2$, R=0.2462.

5.2.2 FEMLAB values

The solution for the FEMLAB setup described in the "Modeling" section is shown in Figure 27 below. Before beginning the simulation process for a LHM, the reflection values from FEMLAB must be compared to the expected values given by the Fabry-Perot equations. For the test simulation the glass slab's physical properties were set to μ=1 and ε=3, and the angle of incidence set to 0°. The equation which determines the electric field intensity after the wave has traveled through the PML is $E_0 = |E_{0z}| e^{-bk_0 \Delta x}$, where E_{0z}=1, b=1, $k_0 = 2\pi/\lambda$=1.5708e+006, and Δx=2.0E-6. Therefore, using the equation and given information, the post PML incident wave amplitude is E_0=0.0432.

The value for $E_0^{'}$ was determined by creating a plot, such as the plot in Figure 26, of the reflected electric field amplitude along the x-axis and using this plot to determine the approximate locations of the wave's peaks; where the coordinates are related through x= x, y=x*tan(2θ)=0. The average of this maximum and the other reflected amplitude values are used in the reflectance calculations.

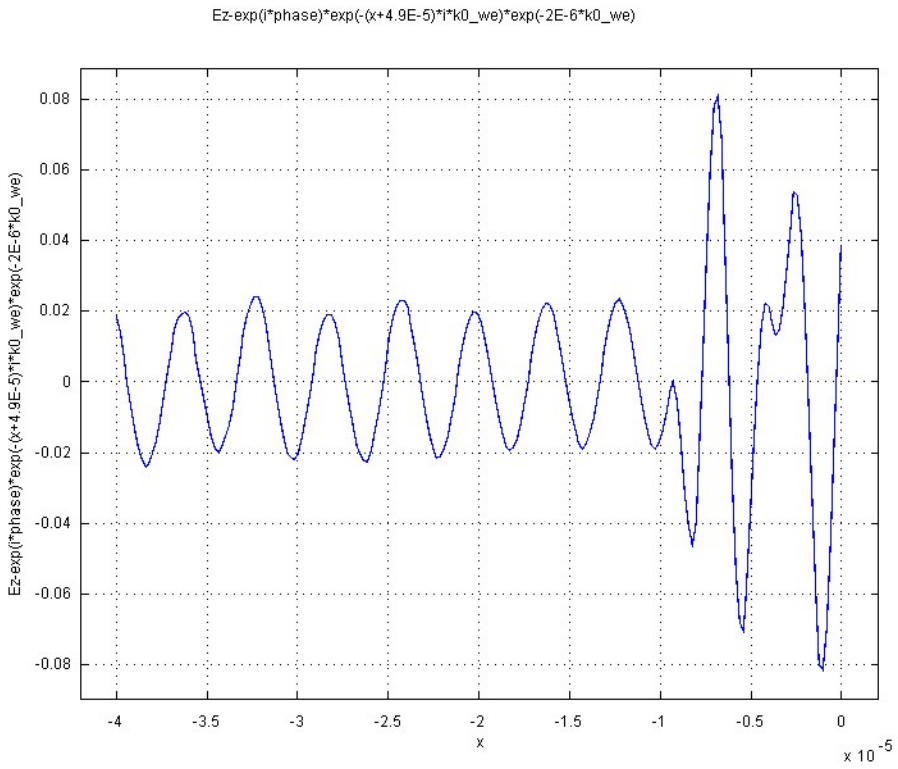

Figure 26: Plot of x vs. reflected wave amplitude at y=0

The next step is to use this data point and the equation $E_z - e^{i*phase}e^{-(x+X1)ik0\_we)}e^{(X2)k0\_we}$ in the "Data display" window found under Post-processing>Data display, the results are given above. After clicking apply, the solution for the equation at the point given above will be displayed at the bottom of the FEMLAB window. Each amplitude value is found and an average of all the values, in the range of x, is used for further calculations. Taking the average also allows the interference, caused by the incident wave interacting with the corners of the slab, to be accounted for. The interference can be seen as fluctuations in the reflected wave amplitude plot. Further justification for taking the average of the amplitudes is given in Appendix A.

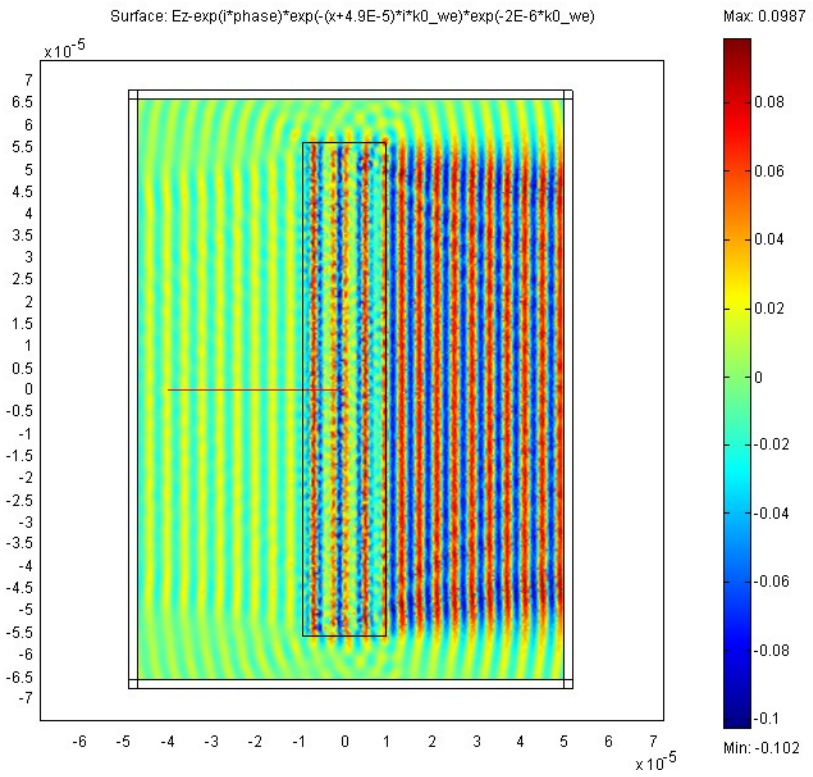

Figure 27: Results of reflected electric field

Figure 27 shows the reflected wave to the left of the slab. The transmitted wave can only be properly visualized by plotting the E_z solution, as shown in a previous section. To the right of the scattered wave image is the wave amplitude scale.

After deriving the Fabry-Perot equations for both $n>0$ and $n<0$, one can calculate the expected reflection results. Using $n = \sqrt{\mu\varepsilon} = \sqrt{3}$, for $n>0$, and $Z = \sqrt{\mu/\varepsilon} = \sqrt{1/3}$, for $n<0$, the expected reflectance values can be calculated as given in Table 7 below.

Angle of incidence	Reflectance value (pos. n value)	Fabry-Perot Reflectance Value (pos. n value)
0	0.2185	0.2462
5	0.2165	0.2437
10	0.2036	0.227
15	0.164	0.1703
20	0.0535	0.0587
25	0.0434	0.0077

Table 7: Positive index of refraction reflectance results

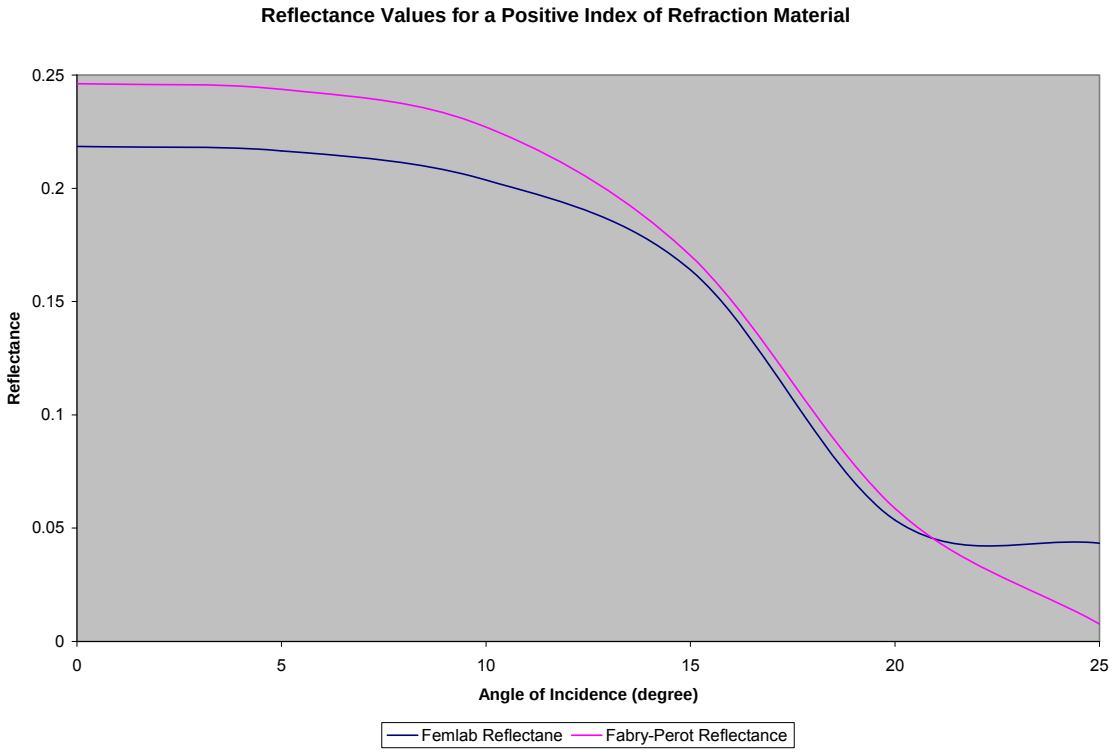

Figure 28: *n*>0 graphical comparison for FEMLAB and Expected Reflectance Values

Figure 28 reveals that the reflectance values determined using the Fabry-Perot equations and those calculated from FEMLAB are very similar.

5.3 LHM Results

During the modeling setup, the value for the incident electric field was set to a value of E_{z0}=1, E_0=0.0432. In order to test the LHM theory, the index of refraction should be set to μ= -1 and ε= -3 by following the steps described in the "Modeling" section. All runs will use an E_{0z} value of one. Calculations for an incidence angle of θ=0º will be shown step by step, but for all other incidence angles, only the results will be presented.

5.3.1 FEMLAB LHM results

After using a stationary linear solver, the default setting found under "Solve>Solver parameters," a wave amplitude plot revealed the E_z values as a function of location. The step-by-step process for determining the reflectance value is the same as the process described in Section 5.1.2. All surface plots will be presented first, and a table of corresponding reflectance values will be presented next. The results for an angle of incidence from 0º to 25 º with a step size of 5º are shown after the sample calculation.

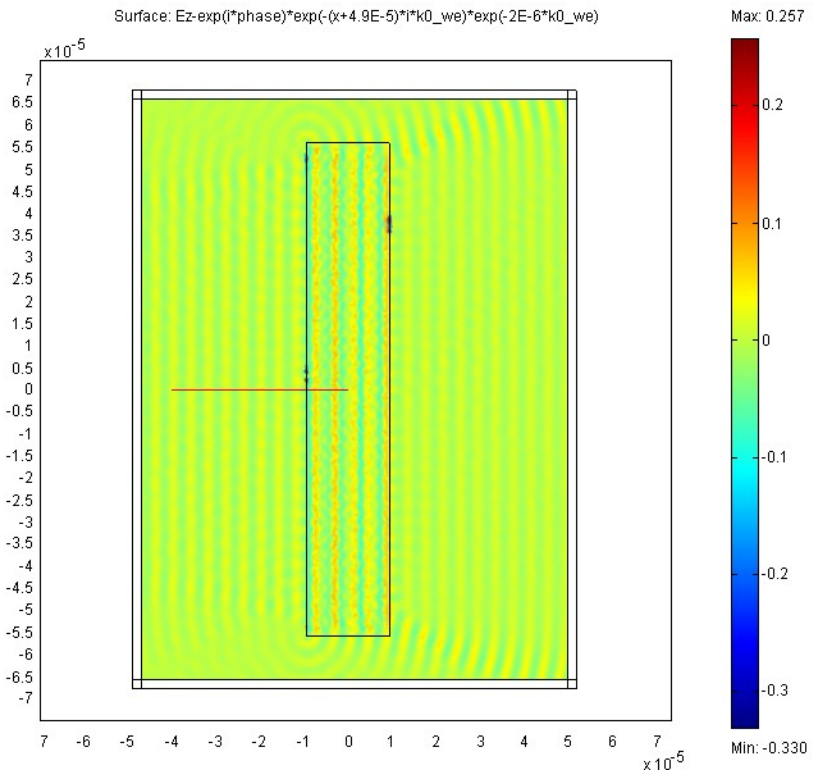

Figure 29: Scattered wave plot of solution using μ= -1 and ε= -3 at 0 degree angle

The figure above shows the scattered wave solution, and the next step is to obtain a plot of x vs. reflectance amplitude. This is done through the use of the "Cross-section Plotting" option and by setting x0= -2E-5, x1=2E-5, y0=x0*tan(2θ), and y1=x1*tan(2θ), where θ is the angle of incidence. Calculations for the y0 and y1 values must be determined outside of FEMLAB and inserted into the boxes.

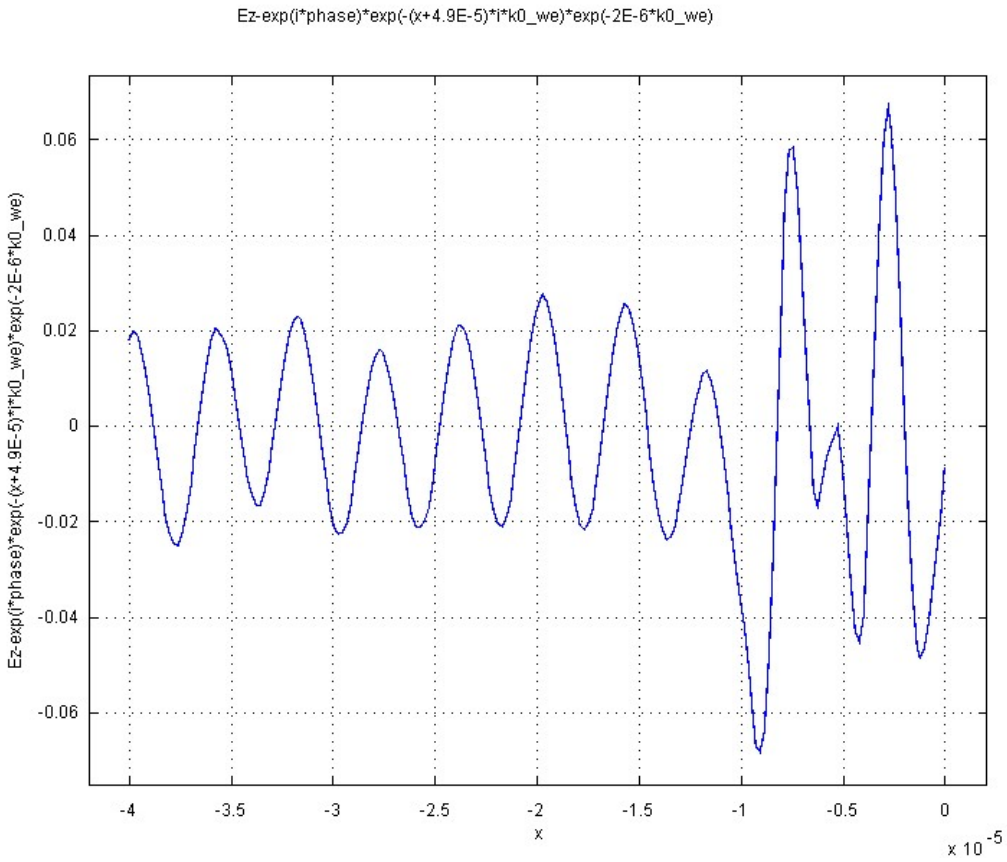

Figure 30: Cross-sectional plot showing amplitude values along x-axis and y=0

Figure 30 depicts the cross-section plot along the x-axis at y=0 for an incidence angle of zero. The location of the amplitudes to the left of the glass slab, x= -1E-5, are determined these location values are entered into the data display. Apply the value at that point is displayed at the bottom of the FEMLAB screen. Each amplitude peak value is found and an average of all the values is used for further calculations.

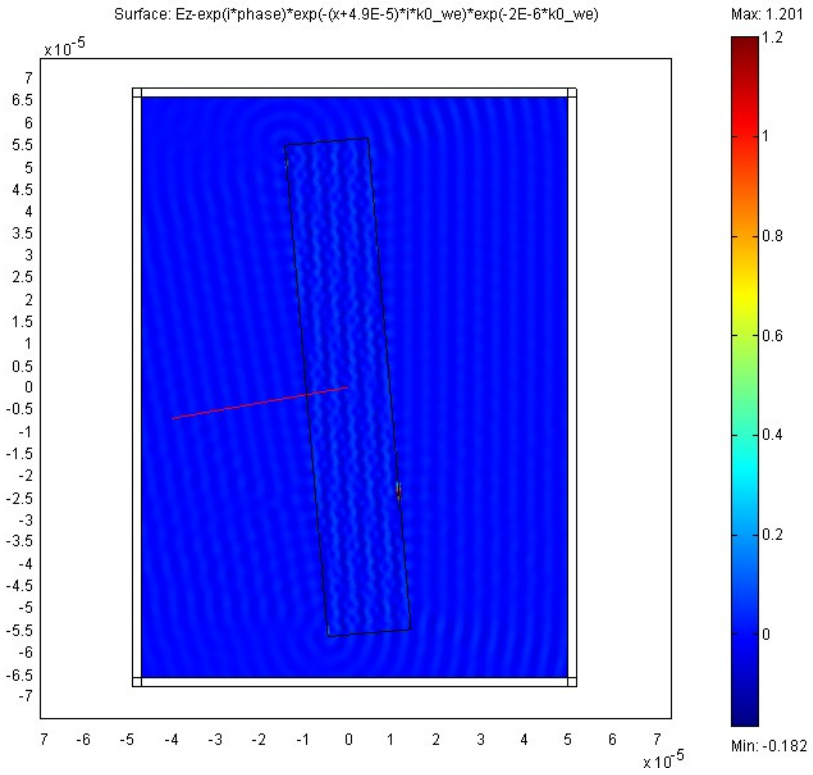

Figure 31: Scattered wave plot of μ= -1 and ε= -3 at 5º incidence

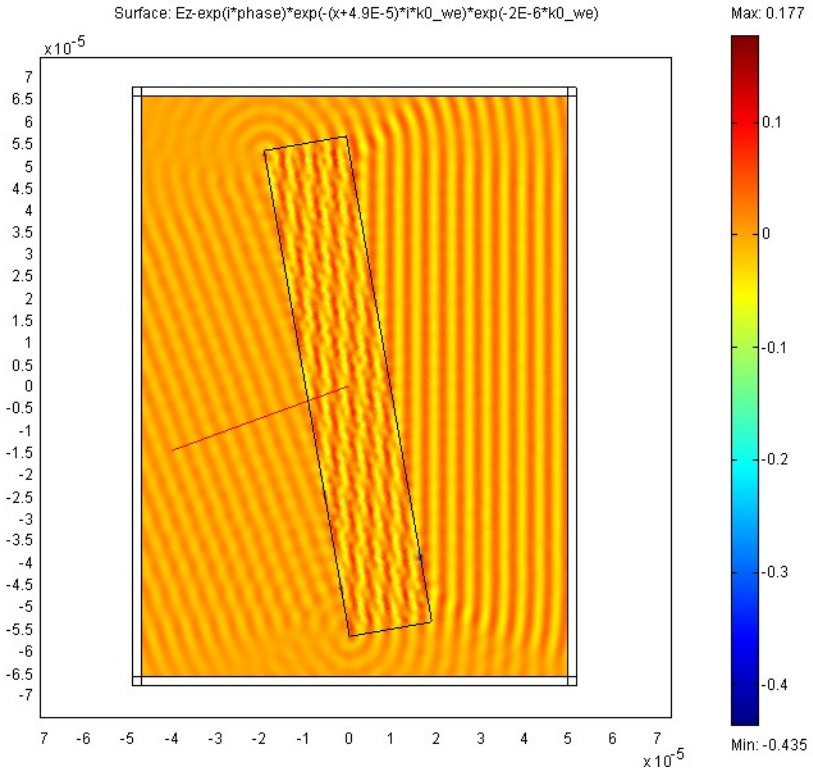

Figure 32: Scattered wave plot of μ= -1 and ε= -3 at 10º incidence

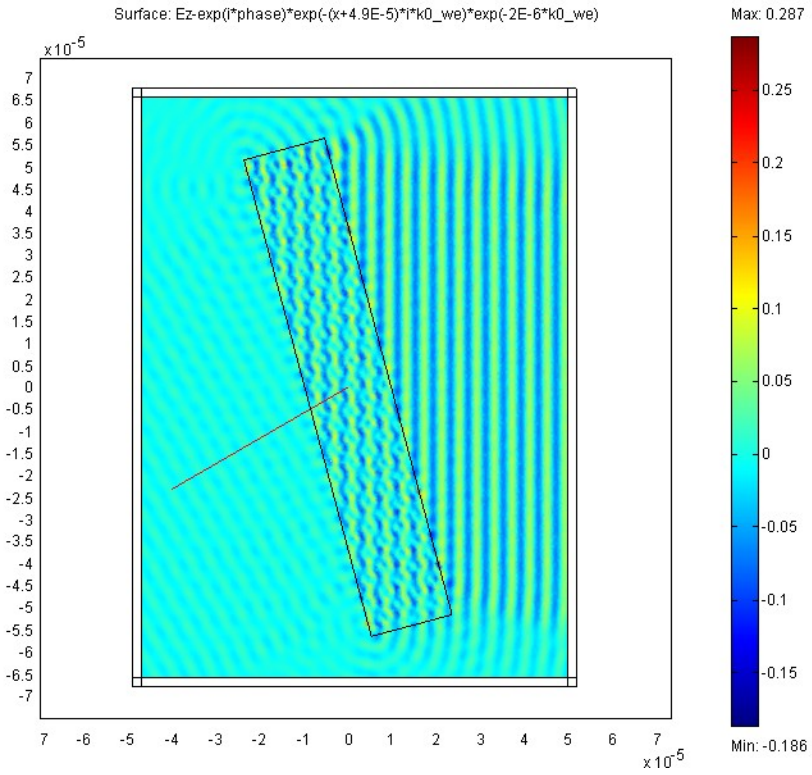

Figure 33: Scattered plot of μ= -1 and ε= -3 at 15º incidence

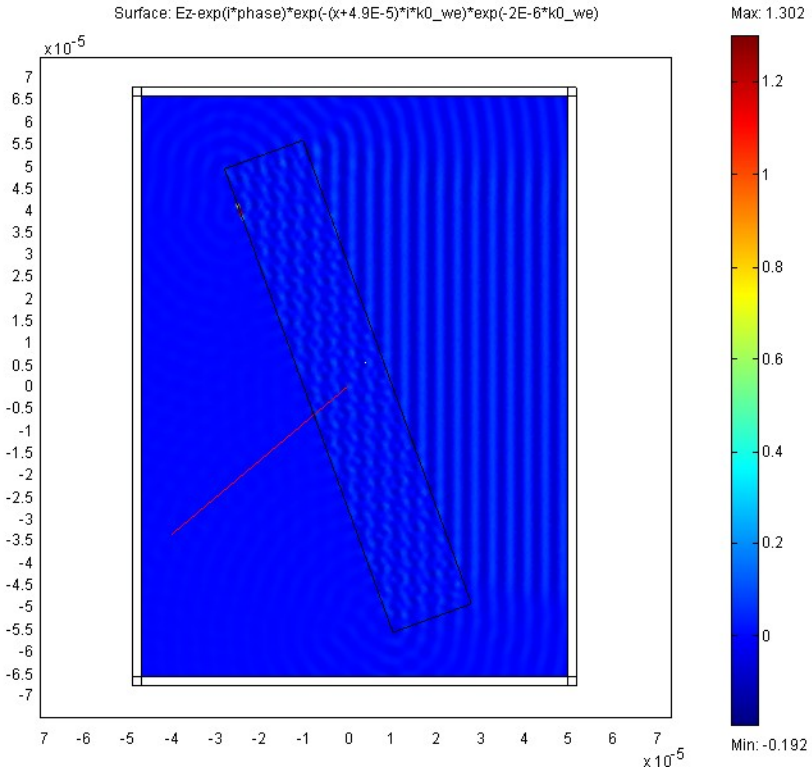

Figure 34: Scattered plot of μ= -1 and ε= -3 at 20º incidence

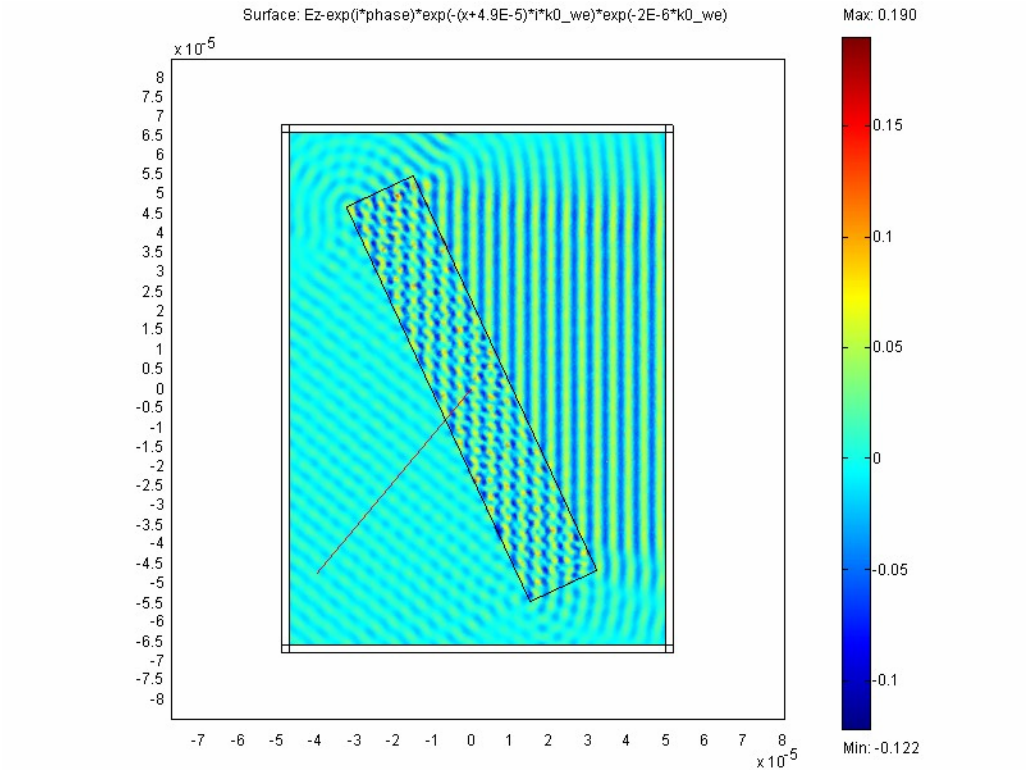

Figure 35: Scattered wave plot of μ= -1 and ε= -3 at 25º incidence

In Figures 31-35, the incident wave is completely vertical. The Law of Reflection states that the angle of incidence is equal to the angle of reflection. The final solution given by FEMLAB proves that the reflected component is found to follow the expected path. The amplitude scale is determined by FEMLAB, and is the reason for the color variation between the scattered wave plots in the figures above. FEMLAB automatically calculates the amplitude scale and plots accordingly.

Please note that as the angle of incidence grows so does the interference caused by the wave interacting with the corners of the slab. The height of the slab and PML was increased to help minimize the interference at the point of calculation. Tables 7 and 8 below reveal the numerical results of a LHM slab and a comparison of the results for the

positive index of refraction and LHM slabs. A graphical comparison of the reflectance values, which reveals similar results, determined using the Fabry-Perot equations and FEMLAB are shown in Figure 36. Please note that in Table 8 the "Reflected E-field amplitude (AVG)" column is the E-field amplitude that was extracted from FEMLAB and inserted into the Fabry-Perot equation.

Angle of incidence	Reflected E-field amplitude (AVG)	Fabry-Perot Reflectance Value (LHM)
0	0.0062	0.2462
5	0.0049	0.2437
10	0.0038	0.227
15	0.0083	0.1703
20	0.0167	0.0587
25	0.024	0.0077

Table 8: FEMLAB and Fabry-Perot reflectance values for $n<0$

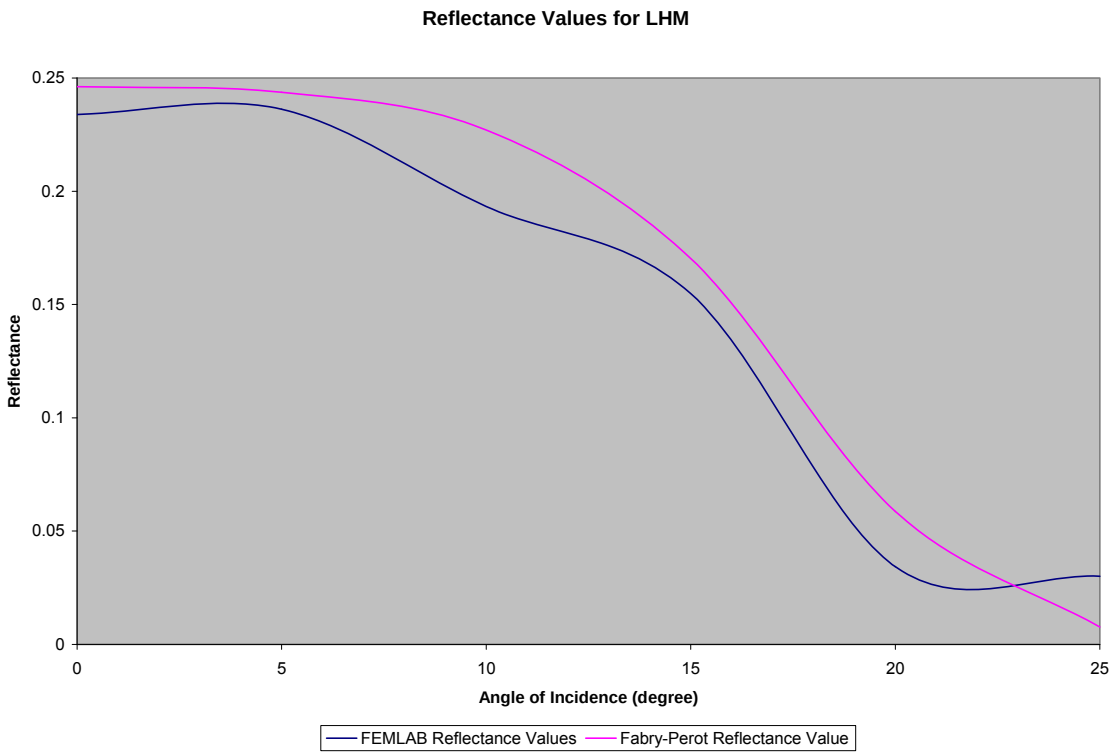

Figure 36: $n<0$ graphical comparison of FEMLAB and expected reflectance values

	FEMLAB		Expected	
Angle of incidence	Reflectance value (pos. n value)	Reflectance Value (LHM)	Fabry-Perot Reflectance Value (pos. n value)	Fabry-Perot Reflectance Value (LHM)
0	0.2185	0.2339	0.2462	0.2462
5	0.2165	0.2362	0.2437	0.2437
10	0.2036	0.1933	0.227	0.227
15	0.164	0.1548	0.1703	0.1703
20	0.0535	0.0343	0.0587	0.0587
25	0.0434	0.0301	0.0077	0.0077

Table 9: Comparison of positive and negative index of refraction reflectance values

Table 9 allows a numerical comparison of the FEMLAB and Fabry-Perot reflectance values. The FEMLAB results, for $n>0$ and $n<0$, show similar reflectance values. The

comparison of FEMLAB (LHM) and Fabry-Perot (LHM) reveal reflectance values whose difference increases as the angle of incidence increases. Such result variation is a result of interference, which is discussed in more depth later in this project.

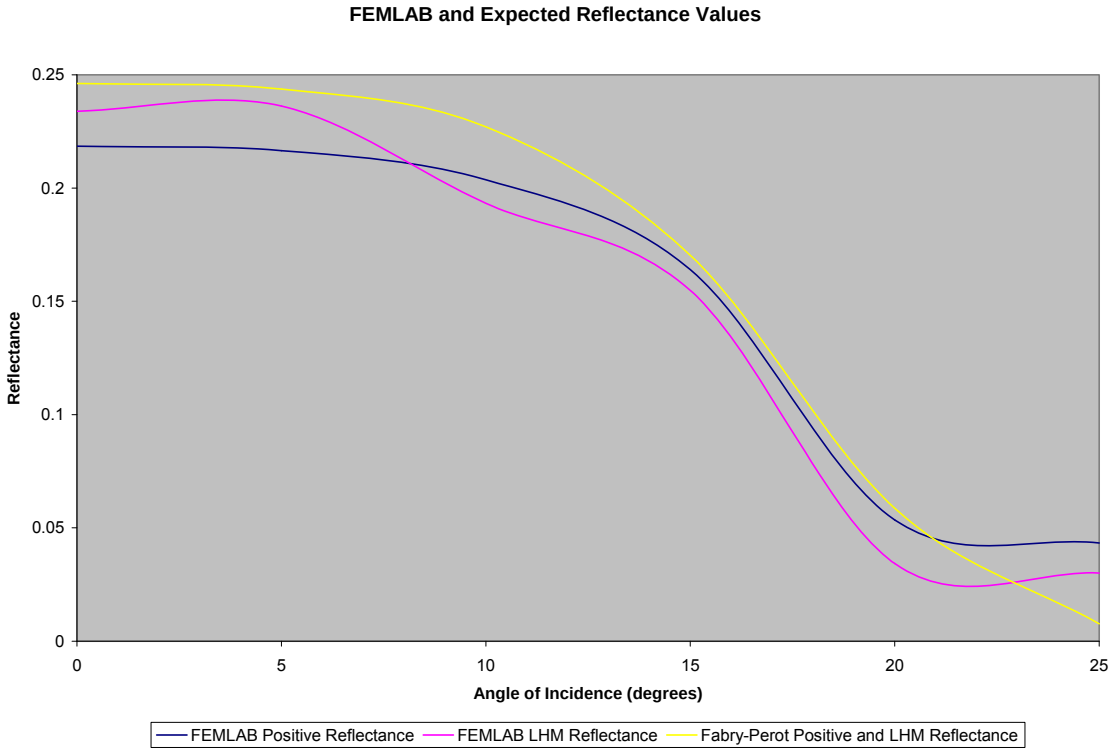

Figure 37: Comparison of $n>0$ $n<0$ for both expected and FEMLAB values

The expected reflectance values should be the same, which they are, as the sign of n should not matter during the expected value calculation [2]. Figure 37 gives a visual comparison of the reflectance values, both FEMLAB and Fabry-Perot. The oscillations seen in the positive FEMLAB reflectance is due to the calculation process and interference. Seeing that the expected reflectance values are the same and the FEMLAB reflectance values are similar, the transmission results will need to be inspected to ensure correct results are obtained from FEMLAB. When a wave is transmitted through an

LHM, it travels on the same side of the normal as the incident wave instead of the crossing the normal at some angle as it does for $n>0$. The angle of refraction at the front face of the slab can be determined using Snell's Law.

Reviewing the reflected wave results, one can see that the FEMLAB values are close but not exact when compared to the expected results. A reason for a slight variation between the expected and FEMLAB values is that unlike the Fabry-Perot equations, FEMLAB does not just give a final single value for the reflectance amplitude. The process of obtaining the peak amplitude value is not perfect and leaves room for error, specifically peak amplitude location and values, during the calculation process.

5.4 Veselago's Theory: *n* vs Z

Physical Law	Equation for nonmagnetic approach	Correct Equation
Snell's Law $n=\sqrt{\varepsilon} \rightarrow n=\sqrt{\varepsilon\mu}$	$n_1 \sin\theta_1 = n_2 \sin\theta_2$	$\frac{\sin\theta_1}{\sin\theta_2} = n_{21} = \sqrt{\frac{\varepsilon_2\mu_2}{\varepsilon_1\mu_1}}$
Fresnel equation $n=\sqrt{\varepsilon} \rightarrow \frac{1}{Z} = \sqrt{\frac{\varepsilon}{\mu}}$	$r_\perp = \frac{n_1\cos\theta_i - n_2\cos\theta_r}{n_1\cos\theta_i + n_2\cos\theta_r}$	$r_\perp = \frac{Z_2\cos\theta_i - Z_1\cos\theta_r}{Z_2\cos\theta_i + Z_1\cos\theta_r}$

Table 10: Corrected equations for selected physical laws

As mentioned earlier, Veselago states that there are groups of physical laws that must be altered to correctly portray situations where $\mu \neq 1$, both uncorrected and corrected equations are given in Table 10 [2]. The first group includes Snell's law, and in [2]

Veselago states that $n = \sqrt{\varepsilon} \rightarrow n = \sqrt{\varepsilon\mu}$. Snell's law retains the *n* notation because *n*<0 when ε, μ<0. The starting for this derivation is the original equations for the incident, reflected, and refracted waves at an interface between two mediums. The equations for these waves were presented earlier while deriving the Fresnel equations. Noting that all three waves have the same frequency, $\omega = 2\pi f = kv$, allows

$$\begin{aligned} kv &= k'v' = k''v'', \\ k &= k'' = \frac{v'}{v}k' = \frac{n}{n'}k'. \end{aligned} \tag{5.3.1}$$

Noting that the boundary conditions state that there must continuity across the interface requires, at z=0,

$$E_0 e^{i(\vec{k}\cdot\vec{r}-\omega t)} + E_0'' e^{i(\vec{k}''\cdot\vec{r}-\omega t)} = E_0' e^{i(\vec{k}'\cdot\vec{r}-\omega t)}. \tag{5.3.2}$$

Looking at the equation, one should see that the boundary conditions require the exponents to be equal due to the fact that the x, y, and t dependencies are confined within them. Setting the exponents equal, at z=0,

$$\begin{aligned} &\vec{k}\cdot\vec{r} = \vec{k}''\cdot\vec{r} = \vec{k}'\cdot\vec{r}, \\ &x(k)_x + y(k)_y = x(k'')_x + y(k'')_y = x(k')_x + y(k')_y. \end{aligned} \tag{5.3.3}$$

The above equation can only be true if the components are separately equal. First setting x=0 and next y=0 reveals

$$\begin{aligned} (k)_y &= (k'')_y = (k')_y, \\ (k)_x &= (k'')_x = (k')_x. \end{aligned} \tag{5.3.4}$$

Placing $\vec{k}$ in the x, z plane forces $(k')_y$=0 and $\vec{k}', \vec{k}''$ to lie within the same plane. The three waves form the plane of incidence which includes the normal to the surface, the z-axis. Applying this to (5.3.4),

$$k \sin \theta_i = k'' \sin \theta_R = k' \sin \theta_T . \tag{5.3.5}$$

Snell's law is also known as the law of refraction explains the path of the transmitted wave. Using (5.3.5) and solving for the transmitted angle with respect to the incident angle,

$$\begin{aligned} n_1 \sin \theta_1 &= n_2 \sin \theta_2 , \\ n_{21} &= \frac{\sin \theta_1}{\sin \theta_2} . \end{aligned} \tag{5.3.6}$$

The next step is to correct the original version of Snell's Law. Converting $n = \sqrt{\varepsilon} \rightarrow n = \sqrt{\varepsilon\mu}$, the corrected equation becomes

$$\frac{\sin \theta_1}{\sin \theta_2} = n_{21} = \sqrt{\frac{\varepsilon_2 \mu_2}{\varepsilon_1 \mu_1}} . \tag{5.3.7}$$

The second group includes the Fresnel equations. Veselago states that the wave impedance must be introduced to these equations, which in turn means Z is introduced into the Fabry-Perot equations also. This correction must be made because Z is always greater than zero when $\varepsilon,\mu<0$. In [2], Veselago claims that "the nonmagnetic approach may lead to incorrect equations, for example, when the condition for the absence of reflection of light on a flat border between two media is considered."

Returning back to the Fresnel Equation derivation, the first step is to look at the boundary conditions once again for a TE wave. The quick derivation was given in an earlier section, but the details will be given below to show how Veselago obtained the corrected version.

$$
\begin{aligned}
&E_0 + E_0^{''} = E_0^{'}, \\
&\sqrt{\frac{\varepsilon}{\mu}}(E_0 - E_0^{''})\cos\theta_i = \sqrt{\frac{\varepsilon'}{\mu'}}E_0^{'}\cos\theta_r .
\end{aligned} \tag{5.3.8}
$$

Noting that $Z = \sqrt{\frac{\mu}{\varepsilon}} = \frac{\mu}{n}$ allows equations (5.3.8) to be written as

$$
\begin{aligned}
&E_0 + E_0^{''} = E_0^{'}, \\
&\frac{1}{Z}(E_0 - E_0^{''})\cos\theta_i = \frac{1}{Z'}E_0^{'}\cos\theta_r , \\
&Z'(E_0 - E_0^{''})\cos\theta_i = Z(E_0 + E_0^{''})\cos\theta_r , \\
&(Z'\cos\theta_i - Z\cos\theta_r)E_0 = (Z'\cos\theta_i + Z\cos\theta_r)E_0^{''}, \\
&\frac{E_0^{''}}{E_0} = r = \frac{(Z'\cos\theta_i - Z\cos\theta_r)}{(Z'\cos\theta_i + Z\cos\theta_r)}.
\end{aligned} \tag{5.3.9}
$$

Theoretically, if this concept is true, only the case where the wave impedance is used should give no reflection between a $n>0$ and $n<0$ medium.

$$
\begin{aligned}
&\varepsilon_1 = 1, \mu_1 = 1, \\
&n_1 = \pm\sqrt{\varepsilon_1\mu_1} = 1, \\
&\varepsilon_2 = -1, \mu_2 = -1, \\
&n_2 = \pm\sqrt{\varepsilon_2\mu_2} = -1.
\end{aligned} \tag{5.3.9}
$$

$$
\begin{aligned}
&n > 0, r = \frac{n_1 - n_2}{n_1 + n_2} = 1, \\
&n < 0, r = \frac{Z_2 - Z_1}{Z_1 + Z_2} = 0.
\end{aligned} \tag{5.3.10}
$$

Equation (5.3.10) above proves that theoretically Veselago's statement in [2] is true. The next step is to verify that FEMLAB is computing the same solution. Figure 38, below, was set up with n=-1, and the scattered wave solution was visualized. The second figure, Figure 39, was given μ= -1 and ε= -1, and the scattered wave solution was also visualized. Notice that FEMLAB also supports Veselago's theory through the fact that a reflection occurred when n was used and no reflection occurred when Z was used in the calculations.

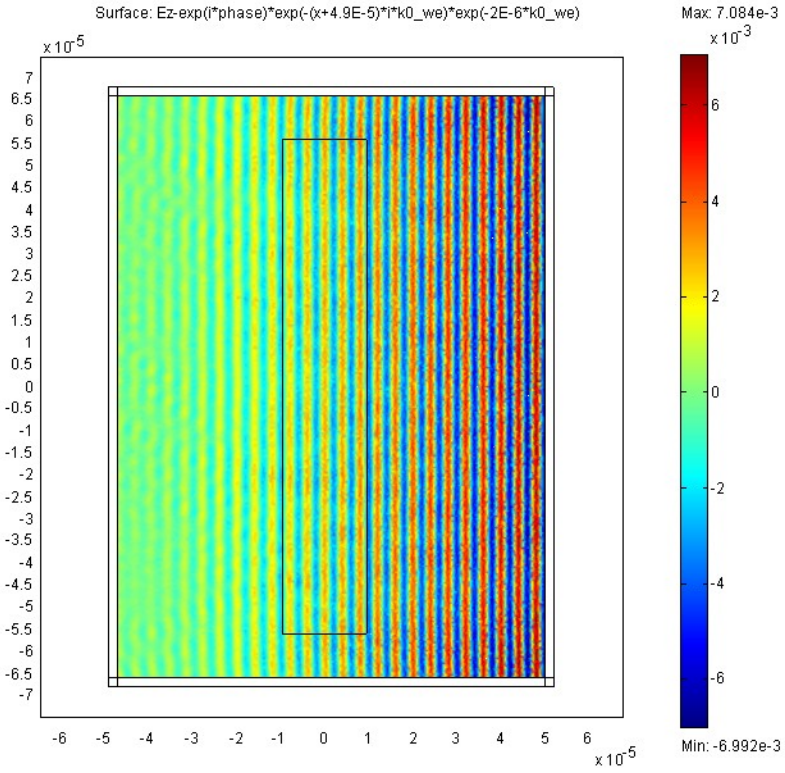

Figure 38: Solution for reflected wave when n=-1 is used in the calculation

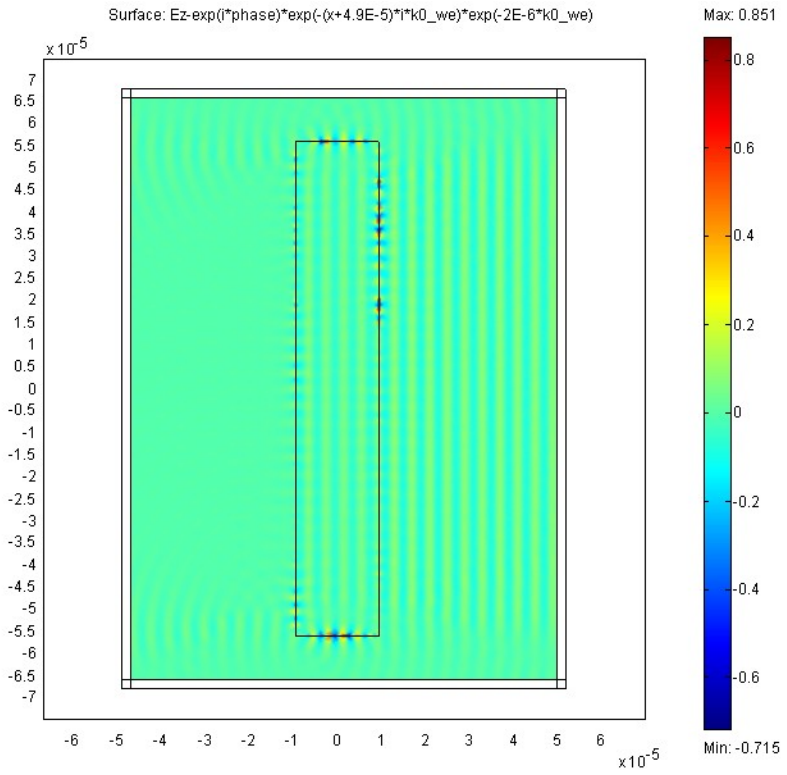

Figure 39: Solution for reflected wave when ε=-1 and μ=-1 are used in the calculation

6 CONCLUSION

The purpose of this project was to inspect the reflective properties and the physics of a left-handed metamaterial (LHM) through the use of FEMLAB. During this process, FEMLAB's ability to visualize and complete calculations using the physical properties of a LHM had to be verified.

The final results of these studies are:

1. FEMLAB does properly reproduce the refraction that occurs as a wave moves from $n>0$ medium to $n<0$ medium.
2. Comparison and calculations show that a LHM, with ε and $\mu<0$, behaves similarly to $n>0$ material for the reflection of an incident wave in the mid-wave infrared region of the electromagnetic spectrum.
3. FEMLAB solution for the proper way to calculate the reflectance of an LHM agreed with Veselago's theory.

Although the expected and FEMLAB values were not exactly the same, they were close and did prove that the reflection of a wave is not effected by a LHM. The results were slightly skewed due to the fact that FEMLAB does not give a single solution for the wave amplitude. Another source for result differences is that the Fabry-Perot equations calculate solutions for an infinite slab, while FEMLAB solves for a finite slab.

The next step in this study might be to introduce a multitude of wavelengths to an LHM and investigate whether the same effects on an incident wave occurs. Two other possibilities are to define the permittivity and permeability as complex values and to determine a more efficient way to model $n<0$ glass slab within FEMLAB. Future analysis may also reveal that the reflectance values calculated using FEMLAB data resemble the expected values more accurately than those computed during this project.

A: PROOF OF NO REFLECTION AT INTERFACE

H_{zx0}=magnitude of magnetic component H_{zx}.

H_{zy0}=magnitude of magnetic component H_{zy}.

E_0=magnitude of electric field

θ= E_0 angle with y-axis

The propagating wave's electric and magnetic field components can be written as [24]

$$\begin{aligned}
\varepsilon_0 \frac{\partial E_x}{\partial t} + \sigma_y E_x &= \frac{\partial (H_{zx} + H_{zy})}{\partial y}, \\
\varepsilon_0 \frac{\partial E_y}{\partial t} + \sigma_x E_y &= -\frac{\partial (H_{zx} + H_{zy})}{\partial x}, \\
\mu_0 \frac{\partial H_{zx}}{\partial t} + \sigma_x^* H_{zx} &= -\frac{\partial E_y}{\partial x}, \\
\mu_0 \frac{\partial H_{zy}}{\partial t} + \sigma_y^* H_{zy} &= -\frac{\partial E_x}{\partial y},
\end{aligned} \tag{A.1}$$

where σ= electric conductivity and σ^*= magnetic conductivity.

$$\begin{aligned}
E_x &= -E_0 \sin\theta e^{i\omega(t-\alpha x-\beta y)}, \\
E_y &= E_0 \cos\theta e^{i\omega(t-\alpha x-\beta y)}, \\
H_{zx} &= H_{zx0} e^{i\omega(t-\alpha x-\beta y)}, \\
H_{zy} &= H_{zy0} e^{i\omega(t-\alpha x-\beta y)},
\end{aligned} \tag{A.2}$$

note that ω= wave pulsation, t= time, and α,β= complex constants.

Assuming that the magnitude E_0 has already been defined, which is an option in FEMLAB, there are only four unknowns to be determined. Using equation groups (A.1) and (A.2) the solutions for α, β, H_{zx0}, and H_{zy0} can obtained.

$$\begin{aligned}
&\varepsilon_0 E_0 \sin\theta - i\frac{\sigma_y}{\omega}E_0 \sin\theta = \beta(H_{zx0} + H_{zy0}),\\
&\varepsilon_0 E_0 \cos\theta - i\frac{\sigma_x}{\omega}E_0 \cos\theta = \alpha(H_{zx0} + H_{zy0}),\\
&\mu_0 H_{zx0} - i\frac{\sigma_x^*}{\omega}H_{zx0} = \alpha E_0 \cos\theta,\\
&\mu_0 H_{zy0} - i\frac{\sigma_y^*}{\omega}H_{zy0} = \beta E_0 \sin\theta.
\end{aligned} \tag{A.3}$$

Using the equations in set (A.3) $\frac{\beta}{\alpha} = \frac{\sin\theta}{\cos\theta}\frac{1 - i(\frac{\sigma_y}{\varepsilon_0\varpi})}{1 - i(\frac{\sigma_x}{\varepsilon_0\omega})}$. In order to ease the simplification process, three new variables will be added.

$$\begin{aligned}
&w_x = \frac{1 - i(\frac{\sigma_x}{\varepsilon_0\varpi})}{1 - i(\frac{\sigma_x^*}{\mu_0\varpi})}, w_y = \frac{1 - i(\frac{\sigma_y}{\varepsilon_0\varpi})}{1 - i(\frac{\sigma_y^*}{\mu_0\varpi})},\\
&G = \sqrt{w_x \cos^2\theta + w_y \sin^2\theta}.
\end{aligned} \tag{A.4}$$

Solving for H_{zx0} and H_{zy0},

$$\begin{aligned}
H_{zx0} &= E_0\sqrt{\frac{\varepsilon_0}{\mu_0}}(\frac{1}{G})w_x \cos^2\theta,\\
H_{zy0} &= E_0\sqrt{\frac{\varepsilon_0}{\mu_0}}(\frac{1}{G})w_y \sin^2\theta.
\end{aligned} \tag{A.5}$$

Combining the solutions for H_{zx0}an H_{zy0} allows H_0 to be written as $H_0 = \frac{E_0}{G}\sqrt{\frac{\varepsilon_0}{\mu_0}}$ (A.6)

Noting that the impedance is simply defined as the magnitude of the magnetic field over the magnitude of the electric field

$$Z = \frac{H_0}{E_0} = \frac{1}{G}\sqrt{\frac{\varepsilon_0}{\mu_0}} \tag{A.7}$$

As long as (σ_x, σ_x^*) and (σ_y, σ_y^*) satisfy the condition $\frac{\sigma}{\varepsilon_0} = \frac{\sigma^*}{\mu_0}$, then the wave components of this scenario can be defined as

$$\Psi = \Psi_0 e^{i\omega(t-(x\cos\theta+y\sin\theta)/cG)} \cdot e^{-\sigma_x \cos\theta/\varepsilon_0 c)x} \cdot e^{(-\sigma_y \sin\theta/\varepsilon_0 cG)y}, \tag{A.8}$$

$$\Psi = \Psi_0 e^{i\omega(t-(x\cos\theta+y\sin\theta)/c)} \cdot e^{-\sigma_x \cos\theta/\varepsilon_0 c)x} \cdot e^{(-\sigma_y \sin\theta/\varepsilon_0 c)y}, \tag{A.9}$$

$$\therefore Z = \frac{\mu_0}{\varepsilon_0}. \tag{A.10}$$

due to the fact that w_x, w_y, G equal unity according to the earlier condition [25]. The first exponential expression in (A.9) shows that the wave phase is propagating in direction normal to the electric field with the speed of light *c*, while the last two exponential expressions regulate the magnitude of the wave.

Looking once again at the PML interface, the incident wave direction will always be perpendicular to the surface of the PML. The total electric and magnetic fields must be continuous across the interface due to imposed boundary conditions. Defining $\vec{E}, \vec{H}$ as being outside the PML and $\vec{E}', \vec{H}'$ being inside the PML, continuity across the interface can be represented as $\begin{matrix}\vec{E} = \vec{E}' \\ \vec{H} = \vec{H}'\end{matrix}$. Knowing that $Z = \frac{\vec{E}}{\vec{H}}$, the statement can be made that the

two impedances, Z and Z' must be equal in order to satisfy the continuity requirement through the following equation, $Z = \frac{\vec{E}}{\vec{H}} = \frac{\vec{E}'}{\vec{H}'} = Z'$, and therefore, no reflections will occur at the interface [25]. Since $Z = \sqrt{\frac{\mu}{\varepsilon}}$ for the PML, the PML/vacuum interface has the same impedance and consequently, using the continuity requirement discussed above, no reflections will occur.

B: AVERAGE PEAK VALUE JUSTIFICATION

During the solution interpretation process, it came to my attention that the reflected wave's amplitude decreased as it traveled through air. Theoretically, the wave should not decay as it travels through air, and this problem needed to be investigated.

Part of the FEMLAB software package included tutorials to help the user learn how to properly use the software [21]. One of these tutorials included a dielectric shape embedded within a PML and surrounded by air. The wavelength in this simulation is λ=0.5. The area enclosed by the PML has been increased in order to see more of the reflected and transmitted waves. If more information on this simulation is desired it can be found in the FEMLAB help file under "Perfectly Matched Layers (PML)." Figure 40 below shows the solution to the FEMLAB run.

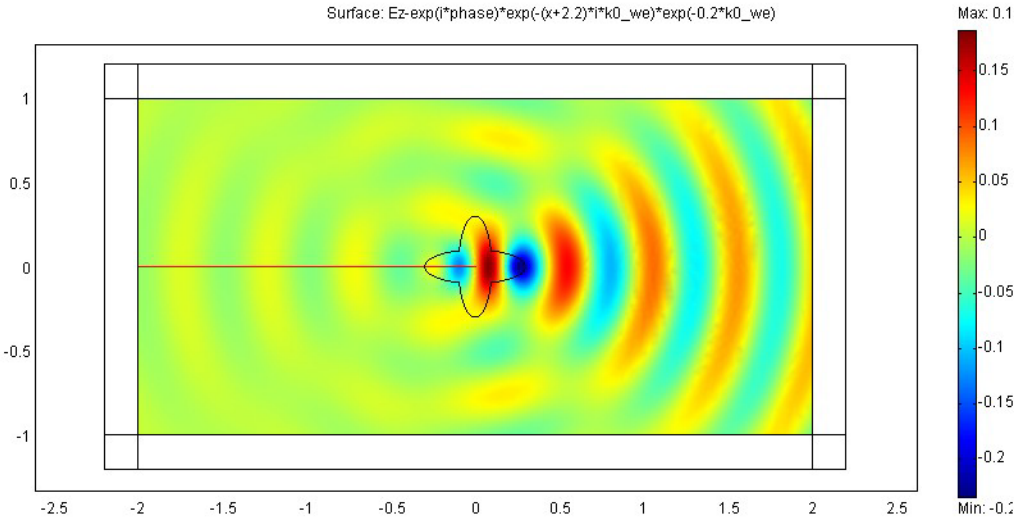

Figure 40: Dielectric solution from FEMLAB tutorial

The red line above represents where the data used to create the cross-sectional plot was acquired.

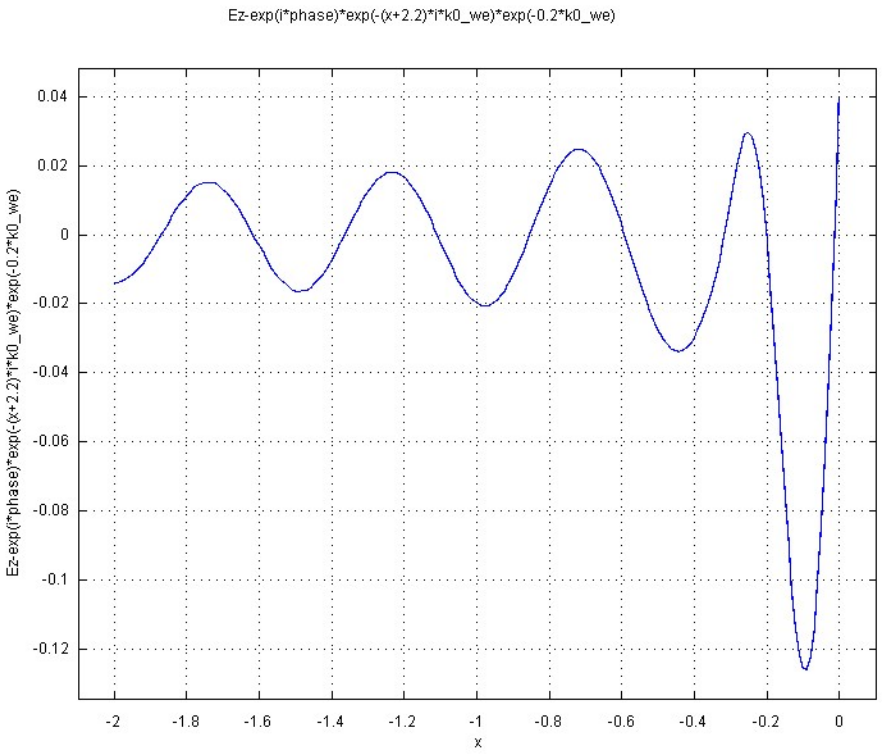

Figure 41: Plot revealing decay of reflected wave

Looking at Figure 41, one can see that as the reflected wave travels back towards the PML the wave is slowly decaying. There is no explanation for this occurrence, as the wave's amplitude should stay the same as it travels through air. Since this phenomenon is seen in the FEMLAB setup used for this report as well as the tutorial supplied by COMSOL one can assume that this will happen in any other similar investigation and is an error of the software. It is because of this decay that the average peak value was used instead of one single peak.

Another reason for taking the average of the peaks was because of the interference caused by the incident wave interacting with the corners of the slab, slab visualization is given in

Figure 42 below. The height of the slab was increased to help minimize any interference from the reflectance value calculation area. The theory in section 5.3 is used here to remove the reflected wave and show the interference caused by the corners and incident wave. Multiple data points were taken along the height of the slab to show that the closer one is to the corner, the more interference will be occurring. The scattered wave solution shows the wave reflected from the corner.

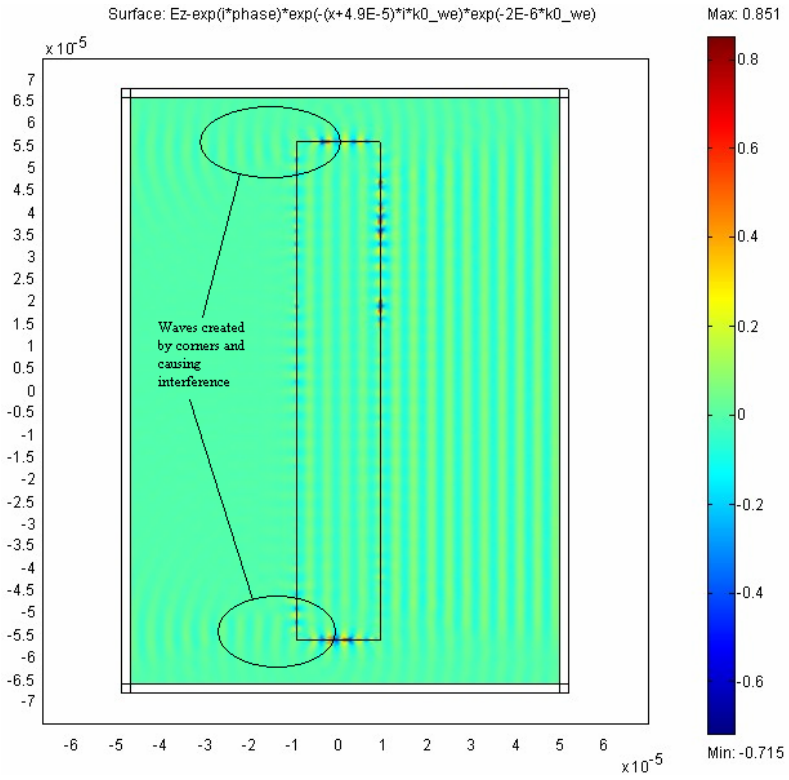

Figure 42: Scattered waves created by incident wave interacting with slab corners

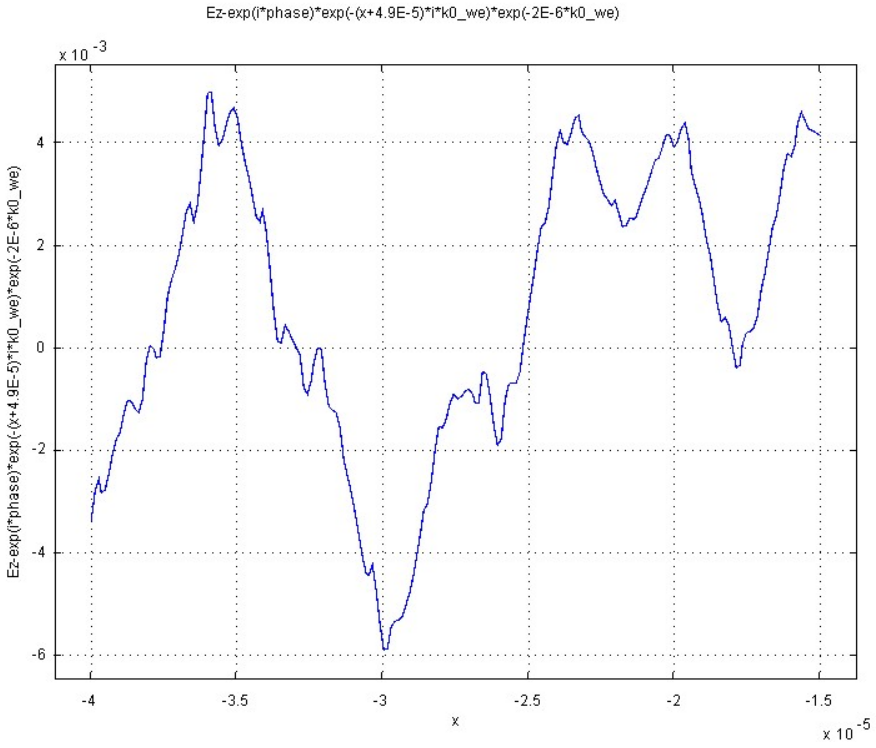

Figure 43: Interference at y=0

Please note that at y=0, interfering waves will be from both top and bottom corners

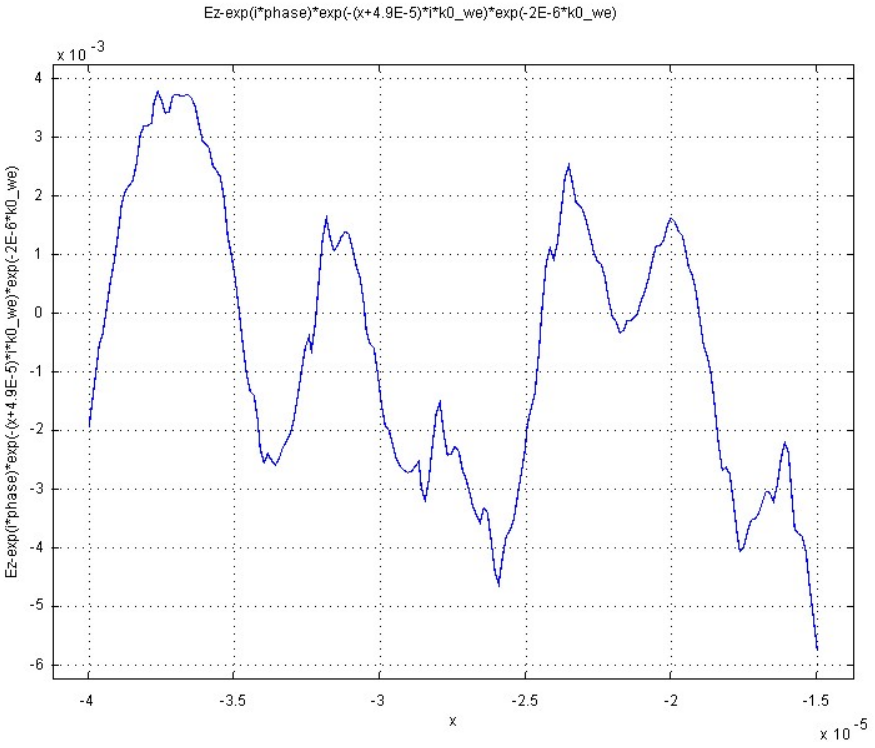

Figure 44: Interference at y=2.5E-5

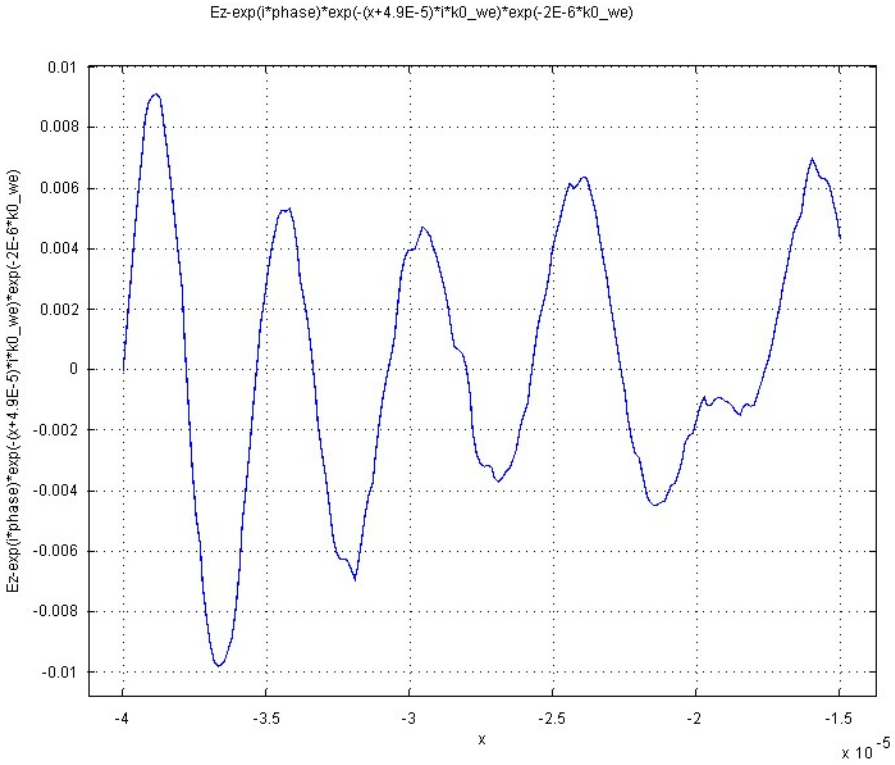

Figure 45: Interference at y=4.0E-5

Figures 44-46 show, as the data point moves up the height of the slab, the interference increases. Figure 46 shows the interference very well. The wave scattered by the corner has an angled path, a product of the interaction, which results in more of this interfering wave being seen further away from the slab.

C: DETERMINING PERMITTIVITY FROM COMPELX PERMEABILITY AND INDEX OF REFRACTION

One of the next steps in investigating a LHM through FEMLAB simulation is to set the index of refraction to a complex value. Introducing an imaginary component into the index of refraction allows the affect of absorption in a LHM to be investigated. The following section explains and derives the value for $\tilde{\varepsilon}_r$ when a material's index of refraction is known. Such a calculation is needed in order to obtain a theoretical reflectance value from Fresnel's equations. The values calculated represent those for medium number two, the glass slab, but will not show the proper notation until the following section.

For an experimental situation involving lossy LHM, one can assume that an absorptive material is used. Such a material's absorption and refraction characteristics can be defined using its complex refractive index, $\tilde{n} = n + i\kappa$, where n is the real part and κ is the extinction coefficient [26]. Setting $\tilde{n} = -1.8 + 0.1i$ allows the complex relative permittivity to be determined. Using the equation, $\tilde{n} = \sqrt{\varepsilon_r \mu_r}$ and setting μ_r=1,

$$\tilde{\varepsilon} = \varepsilon_1 + i\varepsilon_2,$$

$$\varepsilon_1 = n^2 - \kappa^2 = 3.23,$$

$$\varepsilon_2 = 2n\kappa = -0.36, \tag{C.1}$$

$$\tilde{\varepsilon}_r = 3.23 - 0.36i.$$

For the situation of a positive refractive index value of $\tilde{n} = 1.8 + 0.1i$, the same steps as above can be followed to determine the complex values for ε_r and μ_r.

$$\tilde{\varepsilon} = \varepsilon_1 + i\varepsilon_2,$$

$$\varepsilon_1 = n^2 - \kappa^2 = 3.23,$$

$$\varepsilon_2 = 2n\kappa = 0.36, \tag{C.2}$$

$$\tilde{\varepsilon}_r = 3.23 + 0.36i.$$

For the situation where a negative value of μ_r is used, say μ_r= -1, the steps for determining the complex permittivity are shown below.

$$\begin{aligned} &\tilde{n} = \sqrt{\varepsilon_r \mu_r} = \sqrt{i^2 \varepsilon_r}, \\ &\tilde{n}^2 = i\tilde{\varepsilon}_r, \\ &i\tilde{\varepsilon}_r = i\varepsilon_1 - \varepsilon_2. \end{aligned} \tag{C.3}$$

Now solving for ε_1 and ε_2

$$\begin{aligned} &\tilde{n}^2 = i\varepsilon_1 - \varepsilon_2, \\ &(n + i\kappa)^2 = i\varepsilon_1 - \varepsilon_2, \\ &-\varepsilon_2 = n^2 - \kappa^2, \\ &\varepsilon_1 = 2n\kappa. \end{aligned} \tag{C.4}$$

Plugging these values back into the original equation:

$$\tilde{\varepsilon}_r = 2n\kappa i + (n^2 - \kappa^2). \tag{C.5}$$

Comparing this result to the result for a positive μ_r, one can see that the same overall value is obtained for the complex permittivity. This result is important to note because in the mode used for the FEMLAB simulations, FEMLAB assumes that $\mu_r = 1$ and therefore $\tilde{\varepsilon}_r = \tilde{n}^2$.

D: MATLAB ROUTINE

```
%Constants
mu1=1;
mu2=-1;
mu3=1;
eps1=1;
eps2=-3;
eps3=1;
Z1=sqrt(mu1/eps1);
Z2=sqrt(mu2/eps2);
Z3=sqrt(mu3/eps3);
n1=1;
n2=-sqrt(eps2*mu2);
n3=1;
lambda=4*10^-6;
d=1.9*10^-5; %d is the slab thickness
fprintf('The expected values using the Electromagnetic Approach for R
is given below\n')

    theta1=deg2rad(15);
    theta2=asin((n1/n2)*sin(theta1));
    theta3=asin((n2/n3)*sin(theta2));
    k1=(2*pi/lambda)*n1*cos(theta1);
    k2=(2*pi/lambda)*n2*cos(theta2);
```

```
 k3=(2*pi/lambda)*n3*cos(theta3);
    phi=k2*d;
    r12=(Z2*cos(theta1)-
Z1*cos(theta2))/(Z2*cos(theta1)+Z1*cos(theta2));
    r23=(Z3*cos(theta2)-
Z2*cos(theta3))/(Z3*cos(theta2)+Z2*cos(theta3));
    r=(r12+r23*exp(-2*i*phi))/(1+r12*r23*exp(-2*i*phi))
    R=(abs(r))^2


    fprintf('R value from FEMLAB is given below\n')
%Constants
    b=1;
    PMLwidth=2*10^-6;
    k0=2*pi/lambda;
    EFEM=0.0075;
    Eo=exp(-b*PMLwidth*k0) %Incident electric field value after PML
    R2=(abs(EFEM/Eo))^2
```

E: EXTRA NOTES AND HELPFUL HINTS

1. At one point during this report, the slab width was set to 20 μm, and theoretically was seeing no reflection of the incident wave. After some equation manipulation it was determined that the combination of the slab width and wavelength were a "special case" for a Fabry-Perot interface. The supporting calculations are below.

Starting with the Fabry-Perot reflectance equation, and knowing that there is no reflection,

$$r = \frac{r_{12} + r_{23}e^{-2i\phi}}{1 + r_{12}r_{23}e^{-2i\phi}} \Rightarrow R = |r|^2 = 0,$$
$$0 = r_{12} + r_{23}e^{-2i\phi},$$
$$-\frac{r_{12}}{r_{23}} = \cos(2\phi),$$
$$0 = \cos(2\phi) \Rightarrow \phi = m\pi/2.$$

These results mean that m must be an integer for the reflectance to be zero.

Now applying this to the equation for phi:

$$\phi = \frac{2\pi d}{\lambda} n_2 \cos\theta_2,$$
$$\frac{dn_2}{\lambda} = m.$$

After plugging in necessary values, if m is determined an integer there will be no reflectance, such as in the case of d=20 μm, n_2= 1.8, and λ=4 μm.

2. Each time the any dimension or angle in the geometry is altered, the PML must be resuppressed and the geometry must be remeshed before solving.

WORKS CITED

[1] V.G. Veselago, *Usp. Fiz. Nauk* 92, 517 (1967) [*Sov. Phys. Usp.* 10, 509 (1968)

[2] V.G. Veselago, L. Braginsky, V. Shklover, and C. Hafner, *Comp. and Theor. Nanosci.* **3**, 189 (2006)

[3] L. Lew Yan Voon. *Theory: Left-handed Metamaterial* (Class notes, Wright State University, 2006)

[4] R.A. Shelby, D.R. Smith, S. Schultz, *Science* **292** (2001)

[5] D.R. Smith and N. Kroll, *Phys. Rev. Lett.* **85**, 14 (2000)

[6] Y. Takayama and W. Klaus, *Jpn J. Appl. Phys* **41**, 6375-6379 (2002)

[7] C. Luo, S. Johnson, and J. D. Joannopoulos *Appl. Phys. Lett.* **81**, 13 (2002)

[8] Y. Zhang, B. Fluegel, and A. Mascarenhas *Phys. Rev. Lett.* **91**, 15 (2003)

[9] P.F. Loschialpo, D.L. Smith, D.W. Forester, and F.J. Rachford, *Phys. Rev. E* **67**, 025602 (2003)

[10] Eleftheriades, G. V. and Balmain, K.G. *Negative Refraction Metamaterials: Fundamental Principles and Applications* (John Wiley & Sons Inc., New Jersey, 2005)

[11] Engheta, Nader and Ziolkowski, Richard. *Electromagnetic Metamaterials: Physics and Engineering Explorations* (John Wiley & Sons Inc., New Jersey, 2006)

[12] D.R. Smith, W.J. Padilla, D.C. Vier, S.C. Nemat-Nasser, and S. Schultz, *Phys. Rev. Lett.* **84**, 18 (2000)

[13] J.B. Pendry, A.J. Holden, D.J. Robbins, and W.J. Stewart, *IEEE Trans. on Microwave Theory Tech.* **47**, 11 (1999)

[14] C. Soukoulis, S. Linden, and M. Wegener, *Science* **315**, 47-49 (2007)

[15] S. Zhang, W. Fan, N.C. Panoiu, K.J. Malloy, R.M. Osgood, and S.R.J. Brueck, *Phys. Rev. Lett.* **95**, 137404 (2005)

[16] J.B. Pendry, Phys. Rev. Lett. **85**, 3966 (2000).

[17] D. Schurig, J.J. Mock, B.J. Justice, S.A. Cummer, J.B. Pendry, A.F. Starr, and D.R. Smith, *Science* **314**, 977 (2006)

[18] Yeh, Pochi. *Optical Waves in Layered Media* (John Wiley & Sons Inc., New Jersey, 2005)

[19] Hecht, Eugene. *Optics* (Addison Wesley, 2001)

[20] Jin, Jianming. *The Finite Element Method in Electromagnetics* (Wiley-IEEE Press, 2002)

[21] FEMLAB 3.1 Documentation/Tutorial.

[22] Jackson, John David. *Classical Electrodynamics* (John Wiley & Sons Inc., New Jersey, 1999)

[23] Griffiths, David J. *Introduction to Electrodynamics* (Benjamin Cummings, 1998)

[24] Berenger, Jean-Pierre, Journal of Comp. Phy. **114**, 185-200 (1994)

[25] Orfanidis, Sophocles J. *Electromagnetic Waves and Antennas* (Rutgers University, New Jersey, 2004)

[26] Fox, Mark. *Optical Properties of Solids* (Oxford University Press, Great Britain, 2001)